# A Finite Volume Approach For Contingent Claims Valuation

R. Zvan*, P.A. Forsyth†, and K.R. Vetzal‡

University of Waterloo
Waterloo, Ontario
Canada N2L 3G1

October 27, 1999

**Abstract**

This paper presents a nonconservative finite volume approach for solving two-dimensional contingent claims valuation problems. The finite volume method is more flexible than finite difference schemes which are often described in the finance literature and frequently used in practice. Moreover, the finite volume method naturally handles cases where the underlying partial differential equation becomes convection dominated or degenerate. This paper will demonstrate how a variety of two-dimensional valuation problems can all be solved using the same approach. The generality of the approach is in part due to the fact that changes caused by different model specifications are localized. Constraints on the solution are treated in a uniform manner using a penalty method. A variety of illustrative example computations are presented.

**Keywords:** Finite volume, local extremum diminishing, contingent claims, option pricing

**Running Title:** Finite volume approach for valuation

**Acknowledgment:** This work was supported by the Natural Sciences and Engineering Research Council of Canada, the Social Sciences and Humanities Research Council of Canada, and the Centre for Advanced Studies in Finance at the University of Waterloo.

*Department of Computer Science, rzvan@yoho.uwaterloo.ca
†Department of Computer Science, paforsyth@yoho.uwaterloo.ca
‡Centre for Advanced Studies in Finance, kvetzal@watarts.uwaterloo.ca

# 1 Introduction

The valuation of various types of derivative securities is a subject of tremendous importance in modern financial theory and practice. As of December 1998, the global gross market value outstanding of such financial instruments was in excess of $U.S. 3 trillion (BIS 1999). One basic type of derivative is an *option*. These contracts come in a wide variety of flavours. The owner of a *call* option has the right to purchase an underlying asset (such as a stock) for a specified price (called the exercise price or strike price) on or before a specified expiry date. A *put* option is similar except the owner of such a contract has the right to sell. Options which can be exercised only on the expiry date are called *European*, whereas options which can be exercised any time up to and including the expiry date are classified as *American*. In addition, there are various kinds of *path-dependent* options. With a *barrier* option, the contract is nullified if the price underlying asset moves outside a certain range. The payoff of a *lookback* option depends on the highest or lowest value attained by the underlying asset during the life of the contract. Similary, an *Asian* option depends on the average value of the underlying asset over time.

Derivative securities are available both on organized financial exchanges and directly from financial institutions ("over-the-counter"). Currently, approximately 85% of the global derivatives market is in over-the-counter securities (BIS 1999). It is critical for the financial institutions offering such products to have accurate valuation models to assist in: i) determining what prices to charge for the contracts; and ii) hedging the risk exposures which arise from selling the contracts.

In general terms, the standard approach to derivatives valuation begins with specifying a set of state variables which are assumed to affect the value of the contract. In the simple case of an option on a stock, this is most often just the price of the underlying stock itself, resulting in a single factor model. However, nothing precludes the incorporation of additional variables. One candidate is a short-term interest rate. The inclusion of this into a stock option valuation model would obviously result in a two-factor model. Having identified the relevant variables, the next step is to make some assumptions regarding their evolution over time. This is done by specifying a stochastic differential equation for each of the factors, containing both a "drift" term and a "volatility" term. The drift term corresponds to the expected change in the factor, while the volatility term provides a random component to this change. The key insight is that a suitably managed portfolio of existing traded securities (with prices which also depend on the set of factors) can be used to replicate the payoff of the derivative contract. In other words, an identical payoff can be obtained in two ways, either directly from the derivative contract or through replication via an appropriate combination of existing traded securities. By the no-arbitrage principle, these two alternatives must cost the same amount. Roughly speaking, an arbitrage strategy produces an instantaneous risk free profit. For example, suppose that the derivative could be sold for a price which exceeded the cost of replicating it. Then a financial institution could sell the derivative, setting aside part of the proceeds to cover its future liability through the replication strategy and locking in the remainder as an arbitrage profit. This could be done as long as the pricing inequality existed, creating unlimited potential gains with no chance of a loss. The no-arbitrage principle precludes the existence of such opportunities. The application of this concept leads to the conclusion that the price of the derivative security must be equal to the cost of its associated replication strategy.

Mathematically, the result of these economic arguments is a partial differential equation (PDE) which can be solved to determine the value of the derivative security. Interested readers can find detailed treatments of this material in texts such as Wilmott, Dewynne, and Howison (1993), Hull (1997) and Wilmott (1998). For present purposes, a few more observations are in order. First, the same arguments can be applied in more general contexts to determine the value of any contractual claim dependent on the assumed factors, not just a derivative security. For instance, a bond could be valued in a setting where the factors are one or more interest rates. This added generality is reflected in the term "contingent claims", referring to any financial instrument with a value contingent on the relevant state variables. Second, although the volatility components of the factors are always important in the valuation PDEs, the drift terms may not be. If a factor is the price of a traded security, then the drift term of that security is not present in the PDE. However, if a factor is not the price of some traded asset (e.g. an interest rate), then the drift term does appear in the PDE, along with an additional parameter known as the market price of risk for the factor. Finally, although in many cases a single factor model suffices, there are numerous contexts in which a two-factor model is required. As mentioned above, the case of an option on a stock where interest rates are assumed to be random is one example. Others are stock option models with stochastic volatility (i.e. where the volatility of the underlying asset is one of the state variables), two-factor interest rate models, options with payoffs dependent on two underlying assets, and certain kinds of path-dependent options.

The purpose of this paper is to present a general finite volume discretization defined on triangles for the numerical solution of two-factor PDE contingent claims valuation models, and to demonstrate its efficacy on several sample pricing problems. Two-factor pricing problems typically have one or more of the following characteristics:

- accurate solutions are required only in a small region;
- constraints on the solution such as barriers can cause irregular boundary geometries (Pooley, Forsyth, Vetzal, and Simpson 1999);
- the underlying PDE can become convection dominated or degenerate;
- the treatment of boundary conditions is complicated by the fact that the PDE can degenerate to a first-order hyperbolic equation normal to the boundary.

We use a finite volume approach to discretize the PDE model since such an approach naturally handles the above situations.

Our discretization differs from traditional finite volume approaches because it is nonconservative. Since PDEs arising in finance are originally in nonconservative form, our discretization can be applied without manipulating the original PDE. Moreover, the nonconservative discretization often simplifies the treatment of boundaries by allowing one to solve the original equation on portions of the boundary (typically where the value of an underlying factor approaches zero). In such cases, the need for applying boundary conditions on those portions of the boundary is eliminated. This is advantageous because there are often no explicit boundary conditions for valuation problems.

Contingent claims valuation models may become convection dominated or degenerate. For example, in some cases path-dependent option pricing models are degenerate because the diffusion tensor is singular. To ensure the generality of the discretization, a local extremum diminishing (LED) scheme is developed for the convective terms in order to ensure that discrete local maximum and minimum principles hold. The LED scheme is defined on irregular triangular meshes and uses a modified van Leer flux limiter (a previous work (Zvan, Forsyth, and Vetzal 1998b) developed a total variation diminishing scheme for orthogonal grids using the modified van Leer limiter). The LED scheme is compact, i.e. the Jacobian has the same nonzero structure as would result from using a centrally weighted method. Furthermore, diffusion in the underlying PDE can be used to reduce the amount of augmenting diffusion introduced by the scheme.

The PDE for the fair market value of a contingent claim can also be derived using dynamic programming principles (Cox, Ingersoll, and Ross 1985), resulting in a Hamilton-Jacobi-Bellman (HJB) equation. For a rigorous account of existence and uniqueness issues associated with solutions of HJB equations, we refer the reader to Crandall, Ishii, and Lions (1992), and Fleming and Soner (1993). The notion of viscosity solutions is used in the absence of classical solutions for HJB equations. Viscosity solutions of Hamilton-Jacobi equations are analogous to entropy condition satisfying solutions (Oleĭnik 1957) of hyperbolic conservation laws. Note that Hamilton-Jacobi equations are not in conservative form. In the one-dimensional case, it has been shown that monotone numerical schemes will converge to the viscosity solution for a first-order Hamilton-Jacobi equation (Crandall and Lions 1984) and the entropy condition satisfying solution for a hyperbolic conservation law (Harten, Hyman, and Lax 1976). For detailed accounts of the theory of entropy condition satisfying solutions of hyperbolic conservation laws, see LeVeque (1990), Smoller (1994) and Kröner (1997). Recently, the use of LED methods for first-order Hamilton-Jacobi equations has been demonstrated in Barth and Sethian (1998). In view of the success of finite volume methods for conservative problems, it appears that it would be a natural extension to use such approaches for the discretization of the Hamilton-Jacobi-type contingent claims pricing equations. Although we are dealing with essentially linear equations (weak nonlinearity is introduced by American style early exercise contract features), we expect that the finite volume method formulated in this work can be generalized in a straightforward fashion to more complex nonlinear PDEs arising in finance.

In summary, the objective of this work is to formulate a general finite volume method (FVM) which:

- supports the use of unstructured triangular meshes and control volumes constructed using perpendicular bisectors or centroids;
- handles degenerate equations on the boundary without difficulties;
- produces solutions that do not contain spurious oscillations when the PDE is convection dominated or degenerate.

The outline of the paper is as follows. Section 2 provides some background material, including a detailed discussion of why the original PDE can often be solved on the boundary where an underlying factor approaches zero. The sample pricing problems are described in Section 3 and the discretization is presented in Section 4. The results are presented in Section 5 and concluding remarks are provided in Section 6.

# 2 Background

Suppose that the value of a contingent claim $U$ is a function of two state variables ($x_1$ and $x_2$) and time ($t^*$). The time evolutions of $x_1$ and $x_2$ are given by the stochastic differential equations (SDEs):

$$dx_1 = a_1(x_1, x_2, t^*)dt^* + b_1(x_1, x_2, t^*)dW_1 \tag{1}$$

and

$$dx_2 = a_2(x_1, x_2, t^*)dt^* + b_2(x_1, x_2, t^*)dW_2 \ , \tag{2}$$

where $W_1$ and $W_2$ are Wiener processes which are related through their correlation coefficient $\rho$. In these SDEs, the $a$'s are drift terms and the $b$'s are volatility terms.

Following the arguments originally developed in Black and Scholes (1973), and Merton (1973) (and described in texts such as Wilmott et al. (1993), Hull (1997) and Wilmott (1998), a PDE for the value of the contingent claim $U = U(x_1, x_2, t^*)$ can be derived. This PDE has the form:

$$U_{t^*} - \mathbf{V} \cdot \nabla U + (\mathbf{D}\nabla) \cdot \nabla U - rU + P = 0 \ , \tag{3}$$

where $r$ is the risk free interest rate and $P$ is a penalty term which is used to enforce any required constraints (see Zvan, Forsyth, and Vetzal (1998a)). Constraints may arise from contractual specifications such as American style early-exercise features, conversion provisions and call provisions. Effectively, $P$ adds or subtracts value in order to ensure that the constraints are met. Note that in some circumstances $r$ will be a constant parameter, but in other cases it will be a variable (either $x_1$ or $x_2$). We will be solving equation (3) backwards in time from the contract maturity date ($t^* = T$) to the present ($t^* = 0$). Consequently, by letting $t = T - t^*$, we can convert equation (3) into the more familiar form:

$$U_t = -\mathbf{V} \cdot \nabla U + (\mathbf{D}\nabla) \cdot \nabla U - rU + P \ . \tag{4}$$

Equation (4) is simply the two-dimensional convection-diffusion equation with diffusion tensor $\mathbf{D}$ and velocity vector $\mathbf{V}$, along with an exponential decay term due to a discounting effect.

The diffusion tensor $\mathbf{D}$ is symmetric positive semidefinite and is usually a function of the space-like coordinates $x_1$ and $x_2$. Typically, $x_1$ and $x_2$ represent quantities such as asset value or interest rate. In virtually all relevant cases, these are constrained to be nonnegative.

Consequently, we shall assume that $x_1, x_2 \geq 0$. In order to ensure the nonnegativity of $x_1$ and $x_2$, it follows that

$$a_1 \geq 0 \text{ and } b_1 \rightarrow 0 \text{ as } x_1 \rightarrow 0 \ , \tag{5}$$

and

$$a_2 \geq 0 \text{ and } b_2 \rightarrow 0 \text{ as } x_2 \rightarrow 0 \tag{6}$$

in equations (1) and (2). As a result, the computational domain can be restricted to $0 \leq x_1 \leq \infty$ and $0 \leq x_2 \leq \infty$. It also follows from (5) and (6) that

$$(\mathbf{D}\nabla)U \cdot \vec{n} = 0 \tag{7}$$

at $x_1 = 0$ or $x_2 = 0$, where $\vec{n}$ is the outward pointing unit normal to the boundary. Note that the underlying PDE becomes degenerate because there is no diffusion normal to the boundaries at $x_1 = 0$ or $x_2 = 0$. Another consequence of the fact that $x_1$ and $x_2$ cannot become negative is that only outgoing information should be required at $x_1 = 0$ or $x_2 = 0$, i.e.

$$\mathbf{V} \cdot \vec{n} \geq 0 \tag{8}$$

at $x_1 = 0$ or $x_2 = 0$. In general, if $\mathbf{V} \cdot \vec{n} < 0$ or $(\mathbf{D}\nabla)U \cdot \vec{n} \neq 0$ at a boundary, then a Dirichlet condition must be imposed.

In addition to this behaviour on boundaries, in some situations there may be no diffusion in one of the coordinate directions throughout the domain. For instance, certain types of Asian options exhibit this behaviour. In such cases equation (4) is degenerate (with all the usual difficulties).

We can also see that equation (4) is in nonconservative form. This is not an artifact of some manipulation of the PDE, but is a direct consequence of the contingent claims analysis. Since $\mathbf{V}$ is generally an arbitrary function of the coordinates (i.e. the velocity is not determined by a material balance equation as would be typical in computational fluid dynamics applications), it is advantageous in terms of the discretization to leave the convective term in nonconservative form. This will be discussed in detail in the following.

Alternatively, we can write equation (4) as

$$U_t = (-\mathbf{V} - (\nabla'\mathbf{D})') \cdot \nabla U + \nabla \cdot \mathbf{D}\nabla U - rU + P \ , \tag{9}$$

where $\nabla'$ is the transpose of $\nabla$. The diffusion term in (9) is in standard conservative form, which is convenient for integrating by parts in finite element discretizations. This approach was used in Forsyth, Vetzal, and Zvan (1999), and Zvan et al. (1998a). However, there are several disadvantages to this approach. The differentiation of the diffusion tensor may introduce singularities into the effective velocity $(-\mathbf{V} - (\nabla'\mathbf{D})')$ in the interior of the domain. Furthermore, for some financial models a PDE will be solved at the boundaries. In such cases the original nonconservative equation (4) must be discretized at the boundaries in order to ensure the correct flow of information. Discretizing (9) for the interior domain and (4) at the boundary complicates software development (Forsyth et al. 1999) and mesh construction.

As noted above, in many cases $(\mathbf{D}\nabla)U \cdot \vec{n} = 0$ on portions of the boundary. This often leads to misconceptions about what boundary conditions are required there. To clarify this, consider this simple one-dimensional case. Suppose that the state variable is the instantaneous risk free interest rate $r$, which follows a process of the form

$$dr = a(b-r)dt^* + \sigma_r r^c dW_r \tag{10}$$

where $a, b, c$ and $\sigma_r$ are positive parameters, and $W_r$ is a Wiener process. Using standard methods, the PDE for the value of a contingent claim $U(r,t)$ is given by

$$U_t = \frac{1}{2}\sigma_r^2 r^{2c} U_{rr} + (a(b-r) - \lambda\sigma r^c)U_r - rU \ , \tag{11}$$

where $\lambda$ is the market price of interest rate risk. Equation (11) is to be solved on the domain $r \geq 0$. If $U$ represents the value of a bond paying fixed coupons, then $U$ tends to zero as $r \to \infty$. Taking the limit of equation (11) as $r \to 0$ gives

$$U_t = abU_r \ . \tag{12}$$

Since $a, b > 0$, equation (12) degenerates to a first-order hyperbolic equation, with domain of dependence consisting of points in $r \geq 0$. Hence, no boundary condition is required at $r = 0$. In fact, imposing any type of condition other than equation (12) at $r = 0$ would be incorrect. Consequently, the discrete equations should not require any conditions at $r = 0$. Computational schemes with this type of property are common in computational fluid dynamics and have been noted in finance (Sulem 1997).

To solve equation (11) numerically, the infinite domain is truncated. An artificial condition determined by asymptotic analysis or financial reasoning ($U = 0$ in this case as $r \to \infty$) must then be imposed at the maximum interest rate ($r_{max}$) on the computational domain. In practice, if $r_{max}$ is sufficiently large, then the artificial condition has a negligible effect on the solution in the region of interest (Barles 1997). The same cannot be said if an inappropriate boundary condition is imposed at $r = 0$ since this is near the region of interest for this type of valuation problem.

Returning to our general two-factor ($x_1$ and $x_2$) context, equations (7) and (8) hold for the models considered in this paper. Thus, no conditions other than the original PDE need to be imposed along $x_1 = 0$ and $x_2 = 0$. The nonconservative finite volume method used in this work handles such boundaries without difficulty. Note, however, that a suitable finite volume must be constructed for points along the boundary.

# 3 Description of Sample Pricing Problems

## 3.1 Worst of Two Assets

To illustrate the convergence of the method, we will compute the price of a European put option on the worst of two assets ($S_1$ and $S_2$). The holder of this contract has the right to sell the lower-valued of two assets for the specified exercise price on a particular maturity date $T$. This is a simple but important test case because it has a known analytic solution (under standard modelling assumptions). In order to demonstrate the efficiency gains that can be obtained by using an irregular mesh, we will also examine pricing a similar American-style contract. As described above, the difference from the European case is that the holder can exercise the option any time up to and including $T$. This introduces a constraint on the solution. Another distinction from the European case is that in general there are no analytic solutions available for American options.

Let the asset price processes be

$$dS_1 = \mu_1 S_1 dt^* + \sigma_{S_1} S_1 dW_{S_1}$$

and

$$dS_2 = \mu_2 S_2 dt^* + \sigma_{S_2} S_2 dW_{S_2} \ ,$$

where $\mu_1$ and $\mu_2$ are expected rates of return, $\sigma_{S_1}$ and $\sigma_{S_2}$ are volatility parameters, and $W_{S_1}$ and $W_{S_2}$ are Wiener processes with correlation coefficient $\rho$. Defining the gradient operator as

$$\nabla = \begin{pmatrix} \frac{\partial}{\partial S_1} \\ \frac{\partial}{\partial S_2} \end{pmatrix} \ ,$$

the value of an option based on two underlying assets, $U(S_1, S_2, t)$, has the form of equation (4) with

$$\mathbf{D} = \frac{1}{2} \begin{pmatrix} \sigma_{S_1}^2 S_1^2 & \rho\sigma_{S_1}\sigma_{S_2} S_1 S_2 \\ \rho\sigma_{S_1}\sigma_{S_2} S_1 S_2 & \sigma_{S_2}^2 S_2^2 \end{pmatrix}$$

and

$$\mathbf{V} = -\begin{pmatrix} rS_1 \\ rS_2 \end{pmatrix} \ .$$

The payoff function (i.e. terminal condition) for a European put on the worst of two assets is

$$U(S_1, S_2, 0) = \max(K - \min(S_1, S_2), 0) \ , \tag{13}$$

where $K$ is the exercise price. For the analogous American put case, the early-exercise constraint is

$$U(S_1, S_2, t) \geq \max(K - \min(S_1, S_2), 0) \ . \tag{14}$$

The boundary conditions for both the European and American valuation problems are

$$\begin{aligned}
\frac{\partial U}{\partial t} &= \frac{1}{2}\sigma_{S_2}^2 S_2^2 \frac{\partial^2 U}{\partial {S_2}^2} + rS_2 \frac{\partial U}{\partial S_2} - rU + P \text{ as } S_1 \to 0 \ , && (15) \\
\frac{\partial U}{\partial t} &= \frac{1}{2}\sigma_{S_1}^2 S_1^2 \frac{\partial^2 U}{\partial {S_1}^2} + rS_1 \frac{\partial U}{\partial S_1} - rU + P \text{ as } S_2 \to 0 \ , && (16) \\
\frac{\partial U}{\partial t} &= \frac{1}{2}\sigma_{S_1}^2 S_1^2 \frac{\partial^2 U}{\partial {S_1}^2} + rS_1 \frac{\partial U}{\partial S_1} - rU + P \text{ as } S_2 \to \infty \ , \quad S_1 \neq S_2 \ , && (17) \\
\frac{\partial U}{\partial t} &= \frac{1}{2}\sigma_{S_2}^2 S_2^2 \frac{\partial^2 U}{\partial {S_2}^2} + rS_2 \frac{\partial U}{\partial S_2} - rU + P \text{ as } S_1 \to \infty \ , \quad S_1 \neq S_2 \ , && (18) \\
U(S_1, S_2, t) &= 0 \text{ as } S_1, S_2 \to \infty \ , \quad S_1 = S_2 \ . && (19)
\end{aligned}$$

Recalling the discussion in Section 2, conditions (15) and (16) are the limits of the underlying PDE as $S_1 \to 0$ and $S_2 \to 0$, respectively. Condition (17) is deduced from the fact that for fixed $S_1$, the payoff becomes independent of $S_2$ as $S_2 \to \infty$. Thus, all derivatives with respect to $S_2$ vanish as $S_2 \to \infty$. Condition (18) is derived in the same fashion. The Dirichlet condition (19) follows from the payoff function (13). Note that the resulting pricing problem is well-posed since conditions (15) to (18) each have a domain of dependence that falls on the boundary.

## 3.2 Asian Options

As noted previously, Asian option contracts have a payoff which is a function of the average value of an underlying asset price over time. Recently, there has been considerable interest in developing pricing algorithms for both European and American style Asian options (Kemna and Vorst 1990; Hull and White 1993; Rogers and Shi 1995; Barraquand and Pudet 1996; Zvan, Forsyth, and Vetzal 1998b; Chalasani, Jha, Egriboyun, and Varikooty 1998). These contracts provide an interesting test case because they are degenerate (there is no diffusion in one of the space-like dimensions).

Assume that the value of an Asian option is a function of the underlying asset price ($S$), its average ($A$), and time. Let the asset price process be

$$dS = \mu S dt^* + \sigma_S S dW_S \ , \tag{20}$$

where $\mu$ is the expected rate of return, $\sigma_S$ is the volatility parameter, and $W_S$ is a Wiener process. The average of the asset price at any time is defined as

$$A = \frac{1}{t^*} \int_0^{t^*} S(\tau) d\tau \ .$$

In the present context, the diffusion and velocity tensors in equation (4) are

$$\mathbf{D} = \frac{1}{2} \begin{pmatrix} \sigma_S^2 S^2 & 0 \\ 0 & 0 \end{pmatrix} \tag{21}$$

and

$$\mathbf{V} = - \begin{pmatrix} rS \\ \frac{S-A}{T-t} \end{pmatrix} \ , \tag{22}$$

where the gradient operator is defined as

$$\nabla = \begin{pmatrix} \frac{\partial}{\partial S} \\ \frac{\partial}{\partial A} \end{pmatrix} \ .$$

We have assumed here that averaging takes place continuously, but alternative formulations where it is discrete are also used (Dewynne and Wilmott 1995; Zvan, Forsyth, and Vetzal 1999).

Although there are many types of Asian options, we will focus only on the case of a fixed strike call. This contract has the payoff function $U(S, A, t = 0) = \max(A - K, 0)$. The boundary conditions are

$$
\begin{aligned}
\frac{\partial U}{\partial t} &= -\frac{A}{T-t}\frac{\partial U}{\partial A} - rU \text{ as } S \to 0 \ , && (23) \\
\frac{\partial U}{\partial t} &= \frac{1}{2}\sigma_S^2 S^2 \frac{\partial^2 U}{\partial S^2} + rS\frac{\partial U}{\partial S} + \left(\frac{S}{T-t}\right)\frac{\partial U}{\partial A} - rU \text{ as } A \to 0 \ , && (24) \\
\frac{\partial U}{\partial t} &= \frac{1}{2}\sigma_S^2 S^2 \frac{\partial^2 U}{\partial S^2} + rS\frac{\partial U}{\partial S} + \left(\frac{S-A}{T-t}\right)\frac{\partial U}{\partial A} - rU \text{ as } A \to \infty \ , \quad S \neq A \ , && (25) \\
\frac{\partial U}{\partial t} &= \left(\frac{S-A}{T-t}\right)\frac{\partial U}{\partial A} \text{ as } S \to \infty \ , \quad S \neq A \ , && (26) \\
U &= A - Ke^{-rt} \text{ as } S, A \to \infty \ , \quad S = A \ . && (27)
\end{aligned}
$$

With respect to conditions (23) to (25), note that the domain of dependence of the original PDE is on the interior of the domain and the boundary as $A \to 0$, $A \to \infty$ $(A \geq S)$ or $S \to 0$. Condition (26) is deduced from the no-arbitrage jump condition for discretely observed Asian options (Zvan et al. 1999), taking the limit as the observation interval tends to zero. Equation (27) follows from the fact that if $A = S \to \infty$, then the option will surely be exercised.

## 3.3 Convertible Bonds

A convertible bond is a corporate bond with the added feature that the holder has the right to convert the bond into a specified number of shares in the corporation, thereby allowing the holder to gain from increases in the stock's value. There is usually a provision that allows the issuer to force holders to redeem the bonds at a specified price. Firms issue convertible bonds primarily to serve as a form of delayed equity or in order to "sweeten" the debt (Nyborg 1996). A number of models for the valuation of convertible bonds have appeared in the finance literature (Ingersoll 1977; Brennan and Schwartz 1977; Brennan and Schwartz 1980; McConnell and Schwartz 1986; Cheung and Nelken 1994; Ho and Pfeffer 1996).

For present purposes, we will use the two factor model described in Wilmott et al. (1993). The state variables are the instantaneous risk free interest rate $r$ and the price of the issuing firm's stock $S$. The interest rate is assumed to follow a process of the form

$$dr = a(b - r)dt^* + \sigma_r r^c dW_r \ ,$$

where $a$, $b$, $\sigma_r$, and $c$ are positive parameters. The evolution of stock price over time is described by

$$dS = \mu S dt^* + \sigma_S S dW_S \ ,$$

where $\mu$ and $\sigma_S$ are positive parameters. The two Wiener processes $W_r$ and $W_S$ are related through the correlation coefficient $\rho$.

By the usual no-arbitrage arguments we obtain an equation of the form (4) with

$$\nabla = \begin{pmatrix} \frac{\partial}{\partial S} \\ \frac{\partial}{\partial r} \end{pmatrix} ,$$

$$\mathbf{D} = \frac{1}{2} \begin{pmatrix} \sigma_S S^2 & \rho \sigma_S \sigma_r S r^c \\ \rho \sigma_S \sigma_r S r^c & \sigma_r^2 r^{2c} \end{pmatrix} ,$$

and

$$\mathbf{V} = - \begin{pmatrix} rS \\ a(b-r) - \lambda \sigma_r r^c \end{pmatrix} ,$$

where $\lambda$ is the market price of interest rate risk. Recall our earlier observation that the drift terms in the SDEs for the state variables do not matter if that variable is the price of a traded security. In this context, note that $S$ is such a variable and the valuation PDE is independent of $\mu$, the drift parameter for $S$. However, $r$ is not the price of a traded asset, and so the drift parameters for $r$ ($a$ and $b$) do appear in the PDE, along with the market price of risk for this factor.

It is assumed that the holder of the bond can convert the bond at any time into $\omega$ shares of the stock, and that the bond is continuously callable prior to maturity. In other words, the issuer can buy back the bond at any time before maturity for the call price ($C_p$). Equation (4) is solved subject to the terminal condition

$$U(S, r, t = 0) = \max(F, \omega S) , \tag{28}$$

where $F$ is the face value of the bond. Equation (28) simply states that the holder will elect to receive the face value of the bond or $\omega$ shares, whichever is worth more.

The conversion and call provisions introduce two constraints on the value of the convertible. First, if the holder can convert the bond into shares at any time, then the value of the bond cannot be less than the conversion value. This implies

$$U(S, r, t) \geq \omega S . \tag{29}$$

Secondly, the call provision prevents the value of the bond from exceeding the call price since it is optimal for the issuer to call the bonds as soon as their value equals the call price. The constraint introduced by this feature is

$$U(S, r, t) \leq C_p . \tag{30}$$

The boundary conditions for the convertible bond are

$$\begin{aligned}
\frac{\partial U}{\partial t} &= \frac{1}{2}\sigma_r^2 r^{2c} \frac{\partial^2 U}{\partial r^2} + (a(b-r) - \lambda \sigma_r r^c) \frac{\partial U}{\partial r} - rU + P \text{ as } S \to 0 , & (31) \\
\frac{\partial U}{\partial t} &= \frac{1}{2}\sigma_S^2 S^2 \frac{\partial^2 U}{\partial S^2} + ab \frac{\partial U}{\partial r} + P \text{ as } r \to 0 , & (32) \\
\frac{\partial U}{\partial t} &= \frac{1}{2}\sigma_S^2 S^2 \frac{\partial^2 U}{\partial S^2} + rS \frac{\partial U}{\partial S} - rU + P \text{ as } r \to \infty , & (33) \\
U(S, r, t) &= C_p \text{ as } S \to \infty . & (34)
\end{aligned}$$

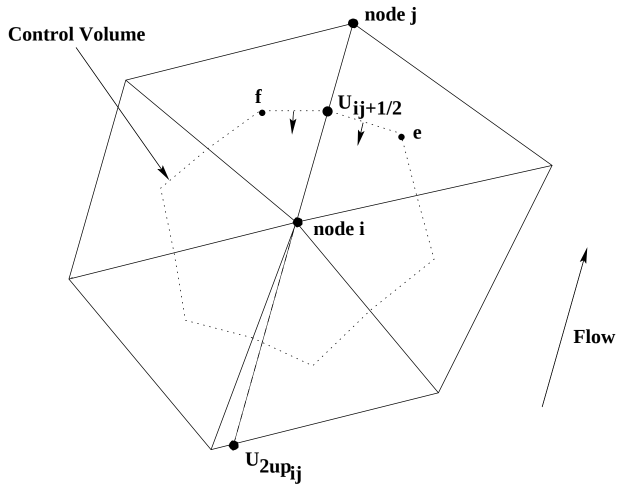


FIGURE 1: *Centroid control volume on a triangulated domain. Points e and f are the centroids of their respective triangles. The face (line segments from e to f) passes through the middle of the edge connecting nodes i and j. $U_{2up_{ij}}$ is the second upstream value.*

Note that equations (31) and (32) are simply the limiting forms of the PDE as $S \to 0$ and $r \to 0$, respectively. Equation (33) is deduced from the fact that the value of a straight bond tends to zero as $r \to \infty$. Thus, the convertible bond derives value (which is capped by the call price) only from the conversion provision (which depends upon $S$) as $r \to \infty$. Equation (34) follows from the call provision. That is, $\omega S \to \infty$ (the conversion value) as $S \to \infty$, but the value of the bond cannot exceed the call price.

Convertible bonds with discrete coupon payments can be modelled using

$$U(S, r, t^+) = U(S, r, t^-) + C \ , \tag{35}$$

where $C$ is the dollar amount of the coupon. In equation (35), $t^+$ and $t^-$ are the times the instant before and after the coupon payment (recall that $t = T - t^*$ is moving backwards in real time).

The above model is of interest numerically for several reasons. First, we have Dirichlet conditions and differential equations on the boundaries. Secondly, there are two (continuously applied) algebraic constraints on the solution. Finally, the underlying PDE becomes degenerate on portions of the boundary.

# 4 Discretization

## 4.1 Nonconservative Finite Volume Method

We will now discretize equation (4) using a nonconservative finite volume method (FVM) defined on a two dimensional computational domain $\Omega$ which is tiled by triangles. We first discuss the treatment of interior nodes.

For a node $i$ in the interior of the computational domain a control volume can be constructed by connecting the midpoints of triangle edges to the triangle centroids (refer to

Figure 1), or by using perpendicular bisectors (Nicolaides 1992) of triangle edges. A centroid construction can always be carried out, but the perpendicular bisector construction requires a Delaunay triangulation. Integrating equation (4) over the finite volume $FV_i$ gives

$$\int_{FV_i} U_t d\Omega = -\int_{FV_i} \mathbf{V} \cdot \nabla U d\Omega + \int_{FV_i} (\mathbf{D}\nabla) \cdot \nabla U d\Omega - \int_{FV_i} rU d\Omega + \int_{FV_i} P d\Omega \ . \tag{36}$$

Let $U_i^{n+1} = U(x_i, y_i, t^{n+1})$. Using fully implicit time stepping for ease of exposition, the following approximations are used for the terms in equation (36)

$$\int_{FV_i} U_t d\Omega \approx A_i \left( \frac{U_i^{n+1} - U_i^n}{\Delta t} \right) , \tag{37}$$

$$-\left( \int_{FV_i} \mathbf{V} \cdot \nabla U d\Omega \right)^{n+1} \approx -\mathbf{V}_i \cdot \oint_{\partial FV_i} U^{n+1} \vec{n} d\Gamma \ , \tag{38}$$

$$\left( \int_{FV_i} (\mathbf{D}\nabla) \cdot \nabla U d\Omega \right)^{n+1} \approx \oint_{\partial FV_i} (\mathbf{D}_i \nabla U^{n+1}) \cdot \vec{n} d\Gamma \ , \tag{39}$$

$$\left( \int_{FV_i} rU d\Omega \right)^{n+1} \approx A_i r_i U_i^{n+1} \ , \tag{40}$$

$$\left( \int_{FV_i} P d\Omega \right)^{n+1} \approx p_i^{n+1} \ , \tag{41}$$

where $A_i$ denotes the area of the finite volume $FV_i$, $\Delta t$ is the time step size, $\Omega_i$ is the set of nodes which are neighbours of node $i$, $\vec{n}$ is the outward pointing unit normal, and $p_i$ is the discrete form of the penalty function (see Zvan et al. (1998a)) used to enforce Dirichlet conditions and constraints. Note that in equations (38) to (40) the integrals have been approximated by evaluating terms which depend on the space-like variables at node $i$. This will be advantageous when dealing with boundary nodes.

Equation (38) is further discretized in the following manner. Let

$$\vec{L}_{ij} = \int_e^f \hat{n} \, d\Gamma$$

where $e$ and $f$ are the endpoints of the face, and $\hat{n}$ is an inward pointing unit normal to the face (refer to Figure 1) between nodes $i$ and $j$. If $U_{ij+\frac{1}{2}}^{n+1}$ is the value at the control volume face separating nodes $i$ and $j$, then equation (38) becomes

$$-\mathbf{V}_i \cdot \oint_{\partial FV_i} U^{n+1} \vec{n} d\Gamma \approx \mathbf{V}_i \cdot \sum_{j \in \Omega_i} \vec{L}_{ij} U_{ij+\frac{1}{2}}^{n+1} \ . \tag{42}$$

The calculation of $U_{ij+\frac{1}{2}}^{n+1}$ will be discussed below in Section 4.2.

Let $N_i$ be the usual $C^0$ Lagrange basis functions defined on triangles where

$$\begin{aligned} N_i &= 1 \ \text{ at node } i \ , \\ &= 0 \ \text{ at all other nodes } , \\ \sum_j N_j &= 1 \ \text{ everywhere in the solution domain } . \end{aligned}$$

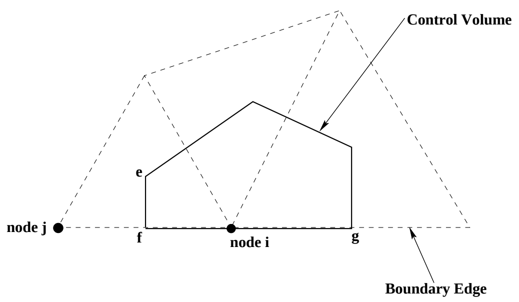


FIGURE 2: *A boundary control volume. The segment $(e, f)$ is the face between nodes $i$ and $j$. The segment $(f, g)$ is the portion of the boundary edge included in order to construct a closed control volume.*

If $U^{n+1} \simeq \sum_j U_j^{n+1} N_j$, then

$$\oint_{\partial FV_i} (\mathbf{D}_i \nabla U^{n+1}) \cdot \vec{n} d\Gamma \approx \sum_{j \in \Omega_i} - \int_\Omega \nabla' N_i \mathbf{D}_i \nabla N_j d\Omega (U_j^{n+1} - U_i^{n+1}) \tag{43}$$

in equation (39). The derivation of approximation (43) is provided in Appendix A.

We have assumed thus far that node $i$ is an interior node. For the case where node $i$ is on the boundary, consider the boundary control volume represented in Figure 2. The construction of boundary control volumes is similar to that of control volumes for interior nodes, except that a portion of the boundary edge must be included in order to construct a closed volume. In other words, in Figure 2 the face denoted by the boundary segment $(f, g)$ must be included. The boundary node has no neighbour for the face $(f, g)$. Without loss of generality, we can assume that $\mathbf{V} \cdot \vec{n} \geq 0$ and $(\mathbf{D}\nabla)U \cdot \vec{n} = 0$ on face $(f, g)$. If either condition is violated, then $i$ must be a Dirichlet node. Hence, an appropriate discretization method will require knowledge of the solution only at points within the computational domain. We can then define the discrete outflow term

$$w_i^{n+1} = \begin{cases} \int_f^g \hat{n} ds \cdot \mathbf{V}_i U_i^{n+1} & \text{if } i \text{ is a boundary node and } \int_f^g \hat{n} ds \cdot \mathbf{V}_i < 0 \ , \\ 0 & \text{otherwise .} \end{cases} \tag{44}$$

Note that for perpendicular bisector control volumes, triangles that contain a boundary edge should contain angles no greater than $\frac{\pi}{2}$ in order to ensure that the control volumes fall within the computational domain (which also prevents self-intersecting control volumes).

Combining approximations (37) to (44) and incorporating a temporal weighting factor $(\theta)$ gives us the following nonconservative finite volume discretization of equation (4)

$$\begin{aligned} A_i \left( \frac{U_i^{n+1} - U_i^n}{\Delta t} \right) = {} & \theta \left( \sum_{j \in \Omega_i} \eta_{ij} (U_j^{n+1} - U_i^{n+1}) + \mathbf{V}_i \cdot \sum_{j \in \Omega_i} \vec{L}_{ij} U_{ij+\frac{1}{2}}^{n+1} - A_i r_i U_i^{n+1} \right) \\ & + (1-\theta) \left( \sum_{j \in \Omega_i} \eta_{ij} (U_j^n - U_i^n) + \mathbf{V}_i \cdot \sum_{j \in \Omega_i} \vec{L}_{ij} U_{ij+\frac{1}{2}}^n - A_i r_i U_i^n \right) \\ & + p_i^{n+1} + \theta w_i^{n+1} + (1-\theta) w_i^n \ , \end{aligned} \tag{45}$$

where $\eta_{ij} = -\int_\Omega \nabla' N_i \mathbf{D}_i \nabla N_j d\Omega$. Setting $\theta$ equal to 1, 1/2, and 0 in (45) respectively produces fully implicit, Crank-Nicolson, and fully explicit schemes.

## 4.2 Convection Dominance and Degeneracy

A standard approach for computing the value $U^{n+1}_{ij+\frac{1}{2}}$ in (45) is to use central weighting

$$U^{n+1}_{ij+\frac{1}{2}} = \frac{U_i^{n+1} + U_j^{n+1}}{2} \ . \tag{46}$$

Such a scheme is second-order accurate, but it can introduce spurious oscillations into the solution if the problem is convection dominated. For example, one cannot ensure that the solution for the hyperbolic equation

$$\frac{\partial U}{\partial t} = -\mathbf{V}(x,y) \cdot \nabla U \tag{47}$$

will be free of spurious oscillations if central weighting is used. An alternative to (46) is first-order upstream weighting, where

$$U^{n+1}_{ij+\frac{1}{2}} = U^{n+1}_{up_{ij}} = \begin{cases} U_i^{n+1} & \text{if } \vec{L}_{ij} \cdot \mathbf{V} < 0 \\ U_j^{n+1} & \text{otherwise} \ , \end{cases} \tag{48}$$

which generally produces solutions of poor quality because of excessive numerical diffusion. If $U_i^{n+1}$ is the upstream point ($U^{n+1}_{up_{ij}}$) in (48), then $U_j^{n+1}$ is referred to as the downstream point ($U^{n+1}_{down_{ij}}$).

Another possibility is to use the flux limiting scheme

$$U^{n+1}_{ij+\frac{1}{2}} = U^{n+1}_{up_{ij}} + \frac{\phi(q^{n+1}_{ij+\frac{1}{2}})}{2}(U^{n+1}_{down_{ij}} - U^{n+1}_{up_{ij}}), \tag{49}$$

where

$$q^{n+1}_{ij+\frac{1}{2}} = \frac{U^{n+1}_{up_{ij}} - U^{n+1}_{2up_{ij}}}{U^{n+1}_{down_{ij}} - U^{n+1}_{up_{ij}}} \tag{50}$$

and

$$\phi(q^{n+1}_{ij+\frac{1}{2}}) = \frac{\left|q^{n+1}_{ij+\frac{1}{2}}\right| + q^{n+1}_{ij+\frac{1}{2}}}{1/\gamma_{ij+\frac{1}{2}} + \left|q^{n+1}_{ij+\frac{1}{2}}\right|} \tag{51}$$

in order to avoid the excessive diffusion of first-order upstream weighting. $U^{n+1}_{2up_{ij}}$ in equation (50) is a convex weighting (i.e. linear interpolation) of $U^{n+1}$ from the two adjacent nodes in the upstream triangle (see Figure 1). In (51),

$$\gamma_{ij+\frac{1}{2}} = \frac{\|(x_{down_{ij}}, y_{down_{ij}}) - (x_{up_{ij}}, y_{up_{ij}})\|}{\|(x_{up_{ij}}, y_{up_{ij}}) - (x_{2up_{ij}}, y_{2up_{ij}})\|}$$

where $\|\cdot\|$ denotes Euclidean length. Equation (51) is known as the van Leer limiter (van Leer 1974; Sweby 1984) and it has been modified to account for nonuniform (irregular) meshes (Zvan et al. 1998b). The modified van Leer limiter (51) has the properties

$$0 \leq \phi(q^{n+1}_{ij+\frac{1}{2}}) \leq 2 \tag{52}$$

and

$$0 \leq \frac{\phi(q^{n+1}_{ij+\frac{1}{2}})}{q^{n+1}_{ij+\frac{1}{2}}} \leq 2\gamma_{ij+\frac{1}{2}} \ . \tag{53}$$

Equation (49) reverts to central weighting when $\phi(q^{n+1}_{ij+\frac{1}{2}}) = 1$ and becomes the two-point upstream scheme

$$U^{n+1}_{ij+\frac{1}{2}} = U^{n+1}_{up_{ij}} + \frac{\gamma_{ij+\frac{1}{2}}}{2}(U^{n+1}_{up_{ij}} - U^{n+1}_{2up_{ij}})$$

when $\phi(q^{n+1}_{ij+\frac{1}{2}}) = q^{n+1}_{ij+\frac{1}{2}}\gamma_{ij+\frac{1}{2}}$.

For one-dimensional problems the flux limiting scheme (49) is local extremum diminishing (LED) (Thuburn 1997) and is total variation diminishing (TVD) for arbitrary temporal weightings if a CFL-like condition is met (Blunt and Rubin 1992; Zvan, Forsyth, and Vetzal 1998b). Equation (49) is a convex weighting of a second-order accurate two-point upstream scheme and central weighting (46). Hence, scheme (49) is second-order accurate except at local extrema where it reverts to a first-order upstream scheme. Unfortunately, TVD schemes can be no more than first-order accurate in two-dimensions (Goodman and LeVeque 1985).

To maintain high order accuracy while ensuring that spurious oscillations are not generated, positive coefficient schemes that are LED have been developed (Spekreijse 1987; Arminjon and Dervieux 1993; Barth 1994; Jameson 1995). In Appendix B, we derive the conditions under which

$$U^{n+1}_{ij+\frac{1}{2}} = \begin{cases} \frac{1}{2}(U^{n+1}_i + U^{n+1}_j) & \text{if } \vec{L}_{ij}\cdot\mathbf{V}(x_i,y_i) \geq 0 \\ U^{n+1}_{up_{ij}} + \frac{\phi(q^{n+1}_{ij+\frac{1}{2}})}{2}(U^{n+1}_{down_{ij}} - U^{n+1}_{up_{ij}}) & \text{if } \vec{L}_{ij}\cdot\mathbf{V}(x_i,y_i) < 0 \end{cases} \tag{54}$$

with arbitrary temporal weighting on an arbitrary triangular mesh produces a positive coefficient (LED) scheme for finite volume discretizations of nonconservative hyperbolic equations such as (47).

A finite volume discretization of equation (47) using (54) is LED if

$$\sum_{j\in\Omega_i}\left(-\bar{\alpha}_{ij}\gamma_{ij+\frac{1}{2}} + \frac{\bar{\beta}_{ij}}{2}\right) \leq \frac{1}{(1-\theta)} \ , \tag{55}$$

where $\bar{\alpha}_{ij} = \frac{\Delta t}{A_i}\min(\vec{L}_{ij}\cdot\mathbf{V}_i, 0)$ and $\bar{\beta}_{ij} = \frac{\Delta t}{A_i}\max(\vec{L}_{ij}\cdot\mathbf{V}_i, 0)$. Condition (55) is a CFL-like condition which is similar to the condition derived in Zvan et al. (1998b) to ensure that (49) produces a TVD scheme for one-dimensional problems on non-uniform orthogonal grids. Condition (55) is trivially satisfied for fully implicit schemes ($\theta = 1$).

The discretization of the full equation (4) using (45) with scheme (54) can be shown to be LED if all the $\eta_{ij}$ ($j \in \Omega_i$) are nonnegative and

$$\sum_{j \in \Omega_i} \left( -\bar{\alpha}_{ij} \gamma_{ij+\frac{1}{2}} + \frac{\bar{\beta}_{ij}}{2} \right) - \bar{\eta}_{ii} \leq \frac{1}{(1-\theta)} \ , \tag{56}$$

where $\bar{\eta}_{ii} = \frac{\Delta t}{A_i} \eta_{ii}$ (note that $-\eta_{ii}$ is positive). However, in general it is not possible to discretize the diffusion operator such that all $\eta_{ij}$ are nonnegative when the diffusion tensor is nonconstant. If some $\eta_{ij}$ are negative, then it cannot be shown that the discretization will be LED. To see this, note that a discretization of the diffusion term (assuming there is at least one Dirichlet node) where some $\eta_{ij} < 0$ will not give rise to an M-matrix. Hence, it cannot be shown that there is a discrete local maximum principle. Nevertheless, the discrete local maximum principle is approximately satisfied as the mesh size parameter tends to zero (refer to Appendix B for a more detailed discussion). It should be emphasized that the effect caused by negative $\eta_{ij}$ is due solely to the diffusion term and is not due to the discretization of the convective term. Appendix B presents alternate schemes that use diffusion in the underlying PDE to reduce the amount of augmenting diffusion that is introduced. The final method is expressed in equation (72) in Appendix B. Flux limiting scheme (72) will be used in the numerical examples.

It is interesting to observe that the Jacobian of the discrete system (45) using scheme (54) (or method (72) derived in Appendix B) has the same nonzero structure as the Jacobian for a centrally weighted discretization (i.e. the scheme is compact). This follows from scheme (54), which is permitted since the original PDE is in nonconservative form. This contrasts with the case of a conservative PDE, where use of a flux limiter results in a large increase in the number of nonzeros relative to a centrally weighted method (Forsyth and Jiang 1997).

## 4.3 Relationship to a Galerkin Finite Element Discretization

Equation (45) can be viewed as a type of finite element discretization. In Appendix C it is shown that the $\eta_{ij} = -\int_\Omega \nabla' N_i \mathbf{D}_{\rm i} \nabla N_j d\Omega$ in discretization (45) are equivalent to the $\eta_{ij}$ which result from using a Galerkin approach with a low order quadrature rule. Although the diffusion term in equation (4) is non-self-adjoint, such a quadrature rule is sufficient for achieving first-order convergence in the $H^1$ norm for self-adjoint elliptic problems using linear elements (Ciarlet 1978). For the sample pricing problems considered in this work, the numerical results in Section 5 indicate second-order convergence for discretization (45).

In addition, the finite volume approximation of the convective term (38) can be viewed as a Galerkin finite element method with a special quadrature rule (Selmin and Formaggia 1996). Approximations (37) and (40) can also be derived by using a Galerkin approach with mass lumping (see Zienkiewicz (1977)) since $A_i = \int_\Omega N_i d\Omega$, if the finite volumes are constructed using triangle centroids.

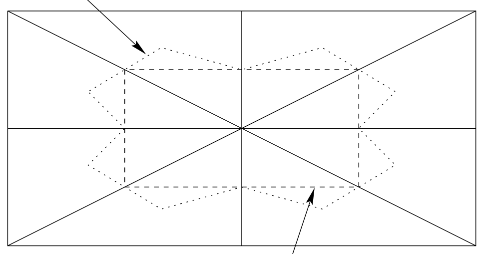


FIGURE 3: *Perpendicular bisector and centroid control volumes.*

# 5 Results

This section provides results for the sample problems described in Section 3 obtained discretizing equation (4) using (45). The runs were performed using ILU-CGSTAB with level one fill. The discrete equations (45) are nonlinear because of the flux limiter (51) or the penalty term. Consequently, full Newton iteration was used to solve the algebraic equations. The Newton iteration tolerance was 0.001 and the inner iteration tolerance was 0.0001. All of the computational domains were chosen such that expanding them had no effect on the solution at the region of interest, to at least five figures. The Crank-Nicolson method ($\theta = \frac{1}{2}$) with a constant time step was used for the computations. In all cases we use parameter values which are typically encountered in practice for the problem under consideration.

All of the triangulations were Delaunay (Lawson 1977) and the control volumes were constructed using perpendicular bisectors (see Figure 3) unless stated otherwise. There is some evidence to suggest that, in some circumstances, centroid control volumes can deteriorate accuracy (Barth 1994). Both methods of control volume construction were examined in the case of convertible bonds.

For the pricing problems in this work, we have only considered the case where the parameters are constant. However, parameters dependent on time or the underlying factors do not introduce any new numerical issues and thus can be easily accommodated. For example, for the case of stock options, volatility can be made a function of time and the underlying stock price (Levin 1998; Coleman, Li, and Verma 1999; Jackson, Süli, and Howison 1999).

## 5.1 Two Asset Options

To demonstrate the convergence of discretization (45) on an irregular mesh (see Figure 4), European put options on the worst of two assets were valued since an analytic solution (Stulz 1982) is known for such problems. Although the underlying PDE is not convection dominated, flux limiting scheme (72) (refer to Appendix B) was used in order to test the full method. The results for European puts with a half year until maturity and various exercise prices ($K$) computed on successively finer irregular meshes (refer to Figure 5) are contained in Table 1. The results demonstrate that numerical solutions of high accuracy (no more than

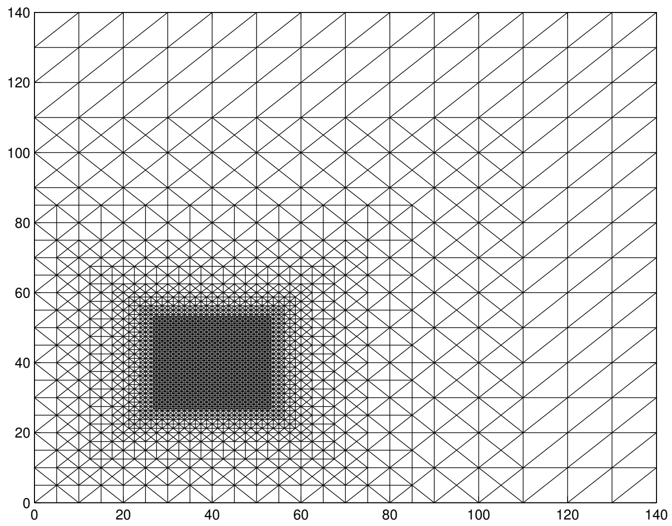


FIGURE 4: *An irregular triangular mesh with 3558 nodes.*

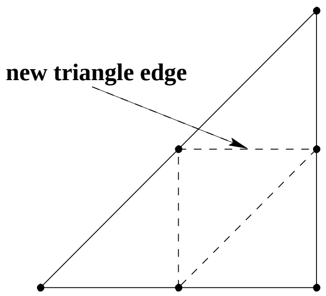


FIGURE 5: *Illustration of mesh refinement. The original triangle is denoted by the solid lines.*

0.006% of the exercise price away from the analytic solution for the cases considered) can be obtained using a mesh with a relatively small number of nodes.

Table 2 contains the values of American put options on the worst of two assets with six months until maturity computed using three alternative schemes: i) the flux limiter (72) on a regular mesh; ii) the flux limiter on an irregular mesh; and iii) central weighting on an irregular mesh. This case differs from the European case above because the early-exercise constraint (14) is being imposed. Regular triangular meshes (see Figure 6) are similar to orthogonal grids (which are typically used when solving PDE models in finance) in the sense that if nodes are added to a region of interest, then the number of nodes in other parts of the domain will also increase. By contrast, irregular meshes allow one to add nodes to the region of interest without increasing the number of nodes in other parts of the domain. Consequently, substantial computational savings can be achieved by using irregular meshes. In this context, the initial irregular mesh (similar to the mesh in Figure 4, but with 2664 nodes) was refined by inserting nodes only near the exercise price. Table 2 indicates that an irregular mesh can be used to price options to within \$0.01 with an order of magnitude less computation time, relative to when a regular mesh is used. The table also shows that

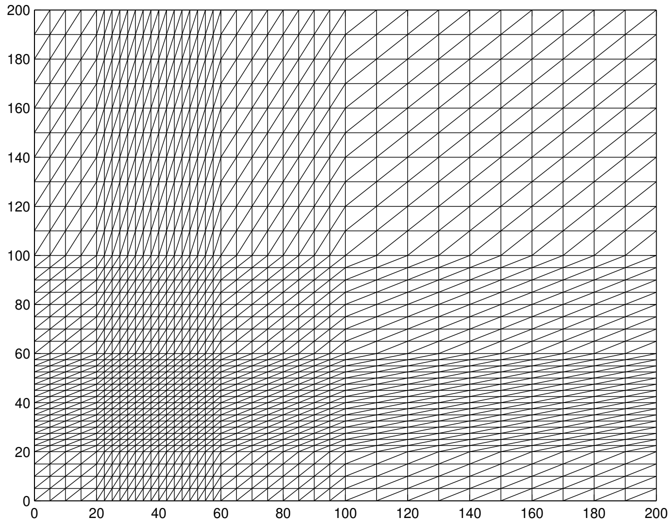



FIGURE 6: *Regular triangular mesh.*

| Nodes | | 3588 | 13140 | 50220 | Analytic |
|---|---|---|---|---|---|
| $\Delta t$ | | 0.02 | 0.01 | 0.005 | |
| | 35 | 1.671 | 1.674 | 1.675 | 1.675 |
| $K$ | 40 | 4.262 | 4.267 | 4.268 | 4.268 |
| | 45 | 7.986 | 7.990 | 7.991 | 7.991 |
| Normalized exec. time | | 1 | 8.11 | 71.60 | |

TABLE 1: *European put options on the worst of two assets when* $r = 0.05$, $\sigma_{S_1} = \sigma_{S_2} = 0.30$, $\rho = 0.5$, $T - t^* = 0.5$, *and* $S_1 = S_2 = 40$. *The solutions were computed on successively finer irregular meshes using the modified van Leer flux limiter. The normalized execution times were obtained by using the coarse grid (3588 nodes and* $\Delta t = 0.02$*) execution time as the base time.*

| | | Regular Mesh Flux Limiter | | | Irregular Mesh Flux Limiter | | Irregular Mesh Central Weighting | |
|---|---|---|---|---|---|---|---|---|
| Nodes | | 5929 | 23409 | 93025 | 2664 | 4744 | 2664 | 4744 |
| $\Delta t$ | | 0.02 | 0.01 | 0.005 | 0.02 | 0.01 | 0.02 | 0.01 |
| | 35 | 1.690 | 1.700 | 1.702 | 1.696 | 1.701 | 1.696 | 1.701 |
| $K$ | 40 | 4.330 | 4.343 | 4.346 | 4.336 | 4.344 | 4.336 | 4.334 |
| | 45 | 8.127 | 8.138 | 8.142 | 8.131 | 8.139 | 8.131 | 8.139 |
| Normalized exec. time | | 1.50 | 12.08 | 82.54 | 1 | 3.63 | 0.97 | 3.47 |

TABLE 2: *American put options on the worst of two assets when* $r = 0.05$, $\sigma_{S_1} = \sigma_{S_2} = 0.30$, $\rho = 0.5$, $T - t^* = 0.5$, *and* $S_1 = S_2 = 40$. *The solutions were computed using the modified van Leer flux limiter on successively refined meshes (both regular and irregular). In addition, solutions were also computed using central weighting on successively refined irregular meshes. The normalized execution times were obtained using the coarse grid (2664 nodes and* $\Delta t = 0.02$*) execution time (when the flux limiter was used) as the base time.*

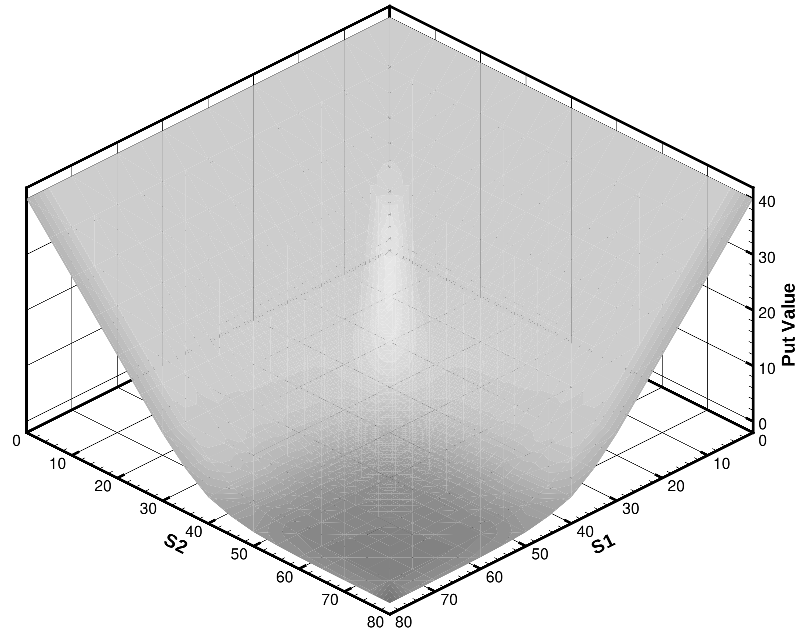


FIGURE 7: *Values for an American put option on the worst of two assets when $r = 0.05$, $\sigma_{S_1} = \sigma_{S_2} = 0.30$, $\rho = 0.5$, $T - t^* = 0.5$ and $K = 40$. The solution was computed on an irregular mesh with 4744 nodes using the modified van Leer flux limiter.*

values computed using central weighting (46) are identical to those obtained using the flux limiting scheme on the same irregular meshes. Scheme (72) uses diffusion in the underlying equation in an attempt to reduce the need for additional numerical diffusion. The results suggest that scheme (72) does indeed introduce little augmenting diffusion. Figure 7 is a plot of American put option values computed using the flux limiting scheme on an irregular mesh.

## 5.2 Asian Options

The values of Asian call options with 3 months until maturity are contained in Table 3. The results were obtained by using scheme (72) on irregular meshes (similar to that in Figure 4). Valuing Asian options is difficult numerically because the underlying PDE is degenerate, having a convection term (see equation (22)) but no diffusion term (see equation (21)) in one of the spatial dimensions. Computing the solution of such a model can be viewed as a standard problem for verifying the robustness of a numerical scheme. The cases considered in Table 3 are particularly difficult because of the low volatility ($\sigma_S = 0.10$). The numerical results are comparable with those obtained using various methods cited in Dempster, Hutton, and Richards (1998).

Figure 8 demonstrates the oscillations that can result when central weighting is used to discretize the convective term. This plot contrasts sharply with Figure 9 which shows the solution obtained using scheme (72) that is free of oscillations. Note that exactly the same parameters and irregular mesh were used to compute both solutions.

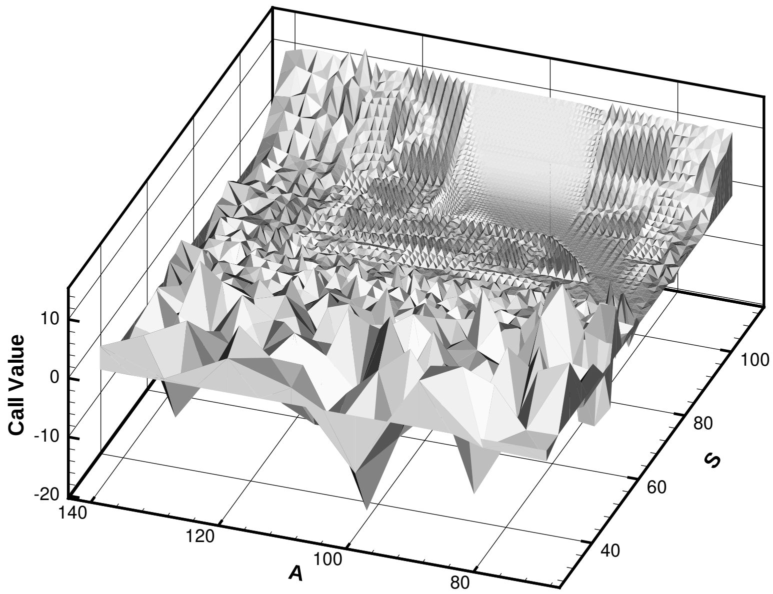


FIGURE 8: *Asian call option value calculated using central weighting on an irregular mesh with 10226 nodes when* $r = 0.10$, $\sigma_S = 0.10$, $T - t^* = 0.25$ *and* $K = 100$.

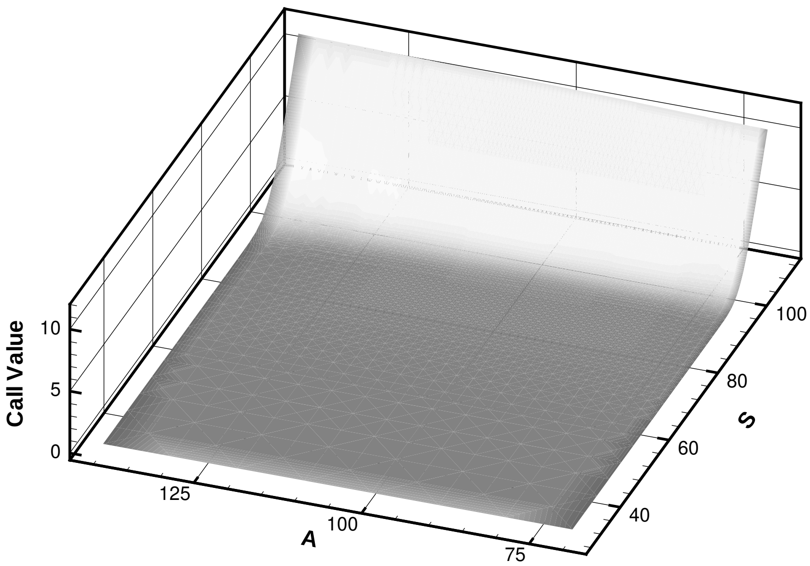


FIGURE 9: *Asian call option value calculated using the modified van Leer flux limiter on an irregular mesh with 10226 nodes when* $r = 0.10$, $\sigma_S = 0.10$, $T - t^* = 0.25$ *and* $K = 100$.

| Nodes | | 2853 | 10226 | 38634 |
|---|---|---|---|---|
| $\Delta t$ | | 0.01 | 0.005 | 0.0025 |
| $K$ | 95 | 6.113 | 6.118 | 6.119 |
| | 100 | 1.829 | 1.848 | 1.852 |
| | 105 | 0.163 | 0.152 | 0.150 |
| Normalized exec. time | | 1 | 7.20 | 69.72 |

Table 3: *Asian call option values computed using the van Leer flux limiter on successively finer meshes when $r = 0.10$, $\sigma_S = 0.10$, $T - t^* = 0.25$, and $S = 100$. The normalized execution times were obtained by using the coarse grid (2853 nodes and $\Delta t = 0.01$) execution time as the base time.*

| Parameter | Value | Parameter | Value |
|---|---|---|---|
| $\sigma_S$ | 0.25 | $c$ | 0.5 |
| $\sigma_r$ | 0.03 | $\lambda$ | 0.0 |
| $\rho$ | -0.5 | $\omega$ | 2.0 |
| $a$ | 0.58 | $Cp$ | 105.0 |
| $b$ | 0.0345 | | |

Table 4: *Convertible bond parameter values.*

## 5.3 Convertible Bonds

In order to compare centroid and perpendicular control volume constructions, we will use both methods to value a ten year convertible bond which is continuously callable and which pays a 5% coupon semi-annually. The parameter values used are shown in Table 4.

Due to the fact that the underlying variables (interest rate $r$ and stock price $S$) differ by orders of magnitude, a rescaling of the variables was necessary in order to construct Delaunay triangulations (which are required for perpendicular bisector control volumes). A new variable $y = \frac{S}{100}$ was defined, and the equations were transformed using it. Note that this type of transformation can only be used in the case of constant stock price volatility.

The values in Table 5 were computed using central weighting and irregular meshes (similar that in Figure 4) with centroid control volumes. Table 6 contains values obtained using flux limiting scheme (72) with centroid control volumes on the same irregular meshes used when the solutions were computed using central weighting. Unlike the solutions above for American put options, there is a noticeable difference here between central weighting and the flux limiting scheme (72), with the flux limiter appearing to be more slowly convergent.

In contrast, Tables 7 and 8 contain values obtained with perpendicular bisector control volumes using central weighting and flux limiting scheme (72) respectively. The values were computed using the same irregular meshes used for the results obtained with centroid control volumes. In this case (using perpendicular bisector control volumes), the values obtained using central weighting and the flux limiting scheme are very similar, and these results are also comparable to the results computed using central weighting with centroid control volumes (Table 5). The results suggest that the differences between the values calculated

| Nodes | | 2698 | 10327 | 40214 | | |
|---|---|---|---|---|---|---|
| $\Delta t$ | | 0.125 | 0.0625 | 0.03125 | | |
| $S$ | 50 | 104.189 | 104.231 | 104.231 | 0.04 | $r$ |
| | 40 | 100.462 | 100.489 | 100.488 | 0.08 | |
| | 30 | 95.095 | 95.128 | 95.123 | 0.12 | |
| Normalized exec. time | | 1 | 8.01 | 122.49 | | |

TABLE 5: *Values of a ten year convertible bond (at $T - t^* = 10.0$) which is continuously callable and pays a 5% coupon semi-annually. The solutions were calculated on successively finer irregular meshes using centroid control volumes and central weighting. The normalized execution times were obtained by using the coarse grid (2698 nodes and $\Delta t = 0.125$) execution time as the base time.*

| Nodes | | 2698 | 10327 | 40214 | | |
|---|---|---|---|---|---|---|
| $\Delta t$ | | 0.125 | 0.0625 | 0.03125 | | |
| $S$ | 50 | 104.189 | 104.231 | 104.231 | 0.04 | $r$ |
| | 40 | 100.428 | 100.471 | 100.479 | 0.08 | |
| | 30 | 95.036 | 95.096 | 95.110 | 0.12 | |
| Normalized exec. time | | 1.32 | 11.38 | 139.49 | | |

TABLE 6: *Values of a ten year convertible bond (at $T - t^* = 10.0$) which is continuously callable and pays a 5% coupon semi-annually. The solutions were calculated on successively finer irregular meshes using centroid control volumes and the modified van Leer flux limiter. The normalized execution times were obtained by using the coarse grid (2698 nodes and $\Delta t = 0.125$) execution time (when central weighting was used (see Table 5)) as the base time.*

| Nodes | | 2698 | 10327 | 40214 | | |
|---|---|---|---|---|---|---|
| $\Delta t$ | | 0.125 | 0.0625 | 0.03125 | | |
| $S$ | 50 | 104.189 | 104.231 | 104.231 | 0.04 | $r$ |
| | 40 | 100.467 | 100.491 | 100.490 | 0.08 | |
| | 30 | 95.097 | 95.132 | 95.129 | 0.12 | |
| Normalized exec. time | | 1 | 7.09 | 102.81 | | |

TABLE 7: *Values of a ten year convertible bond (at $T - t^* = 10.0$) which is continuously callable and pays a 5% coupon semi-annually. The solutions were calculated on successively finer irregular meshes using perpendicular bisector control volumes and central weighting. The normalized execution times were obtained by using the coarse grid (2698 nodes and $\Delta t = 0.125$) execution time as the base time.*

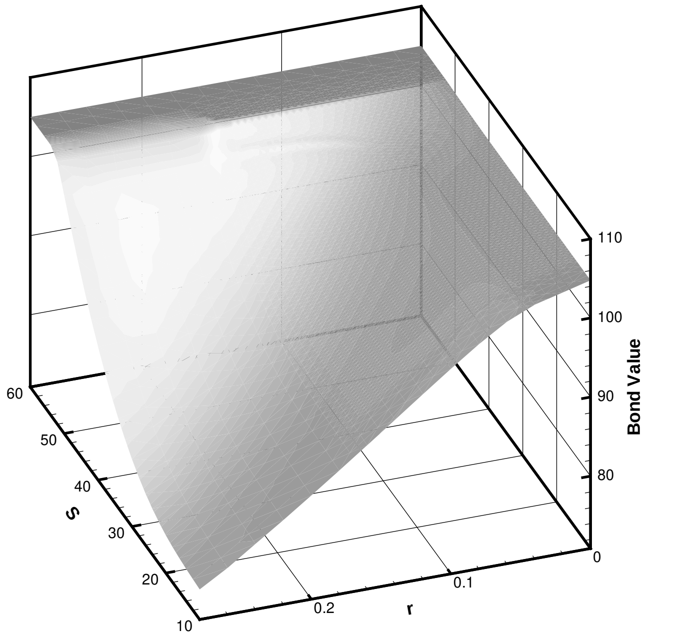


FIGURE 10: *A ten year convertible bond (at $T - t^* = 10.0$) which is continuously callable and pays a 5% coupon semi-annually. The solution was computed on an irregular mesh with 10327 nodes using centroid control volumes and the modified van Leer limiter.*

| Nodes | | 2698 | 10327 | 40214 | | |
|---|---|---|---|---|---|---|
| $\Delta t$ | | 0.125 | 0.0625 | 0.03125 | | |
| $S$ | 50 | 104.189 | 104.231 | 104.231 | 0.04 | $r$ |
| | 40 | 100.465 | 100.490 | 100.489 | 0.08 | |
| | 30 | 95.084 | 95.125 | 95.128 | 0.12 | |
| Normalized exec. time | | 1.13 | 9.57 | 120.28 | | |

TABLE 8: *Values of a ten year convertible bond (at $T - t^* = 10.0$) which is continuously callable and pays a 5% coupon semi-annually. The solutions were calculated on successively finer irregular meshes using perpendicular bisector control volumes and the modified van Leer flux limiter. The normalized execution times were obtained by using the coarse grid (2698 nodes and $\Delta t = 0.125$) execution time (when central weighting was used (see Table 7)) as the base time.*

with centroid control volumes were due to the fact that such control volumes had a diffusive effect on the solution, primarily when the flux limiting scheme was used. This is most likely due to the fact that the shape of the centroid control volumes (see Figure 3) increased the usage of the flux limiter.

Figure 10 contains a plot of the convertible bond values computed using scheme (72) on an irregular mesh. In this figure, the effect of the call provision (constraint (30)) can clearly be seen for large $S$.

# 6 Conclusions

We have described a general finite volume framework for two-factor contingent claims PDE valuation models. In order to ensure generality, a nonconservative finite volume method was formulated. This method is specifically designed to handle degenerate equations (especially at boundaries) and convection dominated situations.

It is often the case that financial valuation problems are posed without explicit boundary conditions. At large (but finite) values of the independent variables in the computational domain, asymptotic forms can usually be used to specify artificial boundary conditions. Since the nodes where these conditions are imposed are usually far from regions of interest, any errors in the asymptotic form will typically have a negligible effect. However, inappropriate boundary conditions near zero may prevent convergence to the true solution in the area of interest because of its proximity to these conditions. It is often the case that on the boundary near the origin, the domain of dependence of the underlying PDE is on the interior domain and boundary. Hence, an appropriate discretization will not need to impose conditions on these portions of the boundary. The nonconservative finite volume approach presented in this work handles such boundary points correctly.

To ensure the robustness of the framework, the prevention of spurious oscillations caused by convection dominance was addressed in this work. In the case of a pure convection problem, this method is local extremum diminishing on an unstructured mesh. A combination of central weighting and a flux limiter is employed, which is possible since the equations are nonconservative. In the case of the complete problem with convection and diffusion, the scheme minimizes the use of the flux limiter, reducing the amount of additional numerical diffusion. Furthermore, this method is a compact scheme, where the nonzero structure of the Jacobian matrix is no different from that obtained when central weighting or first-order upstream weighting is used.

The numerical examples presented in this work indicate that the use of the flux limiting scheme is superior to central weighting for degenerate or convection dominated cases. On the other hand, when there is enough diffusion in the problem so that central weighting can be used, both methods give comparable results, particularly if the control volumes are constructed using perpendicular bisectors. However, if centroid control volumes are used, then there is some degradation in accuracy when the flux limiting scheme is employed. To summarize, if a Delaunay triangulation can be constructed, then the flux limiting scheme is a robust method which produces good results in degenerate cases, and is comparable to central weighting when that approach can be used.

Although the computational domains for contingent claims valuation problems are typically rectangular, accurate solutions are only required in a small subregion near the exercise price. As demonstrated in the numerical examples, an unstructured grid is very useful in such cases, since more nodes can be inserted near the region of interest without introducing additional nodes elsewhere in the computational domain.

The framework presented in this work differs from the approach that is often employed in the finance literature, where a separate numerical technique is developed for each class of valuation model. We have demonstrated that many two-factor cases can be priced using the same general framework. The discretization method used in this work does not require special knowledge of the details of any particular valuation model. The general approach allows for the development of software that isolates model specifications. For example, in an object-oriented implementation, model classes can be developed which specify the velocity and diffusion tensors, boundary conditions and constraints. Thus, different financial claims can be valued by simply constructing new classes. No other modifications to the software are required.

# Appendices

## A Nonconservative Finite Volume Approach for Diffusion

In this Appendix, we will derive expression (43), the discretization of the diffusion term. Let $T_i$ be the set of triangles with node $i$ as a vertex and $FV_i^m$ be the portion of the control volume associated with node $i$ in triangle $m$ ($\Delta_m$). Then equation (39) becomes (dropping time dependence)

$$\oint_{\partial FV_i} (\mathbf{D}_i \nabla U) \cdot \vec{n} d\Gamma = \sum_{\Delta_m \in T_i} \int_{\partial FV_i^m} (\mathbf{D}_i \nabla U) \cdot \vec{n} d\Gamma \ . \tag{57}$$

With reference to Figure 11, let $\nabla U = \sum_{j \neq i} \nabla N_j^m (U_j - U_i)$, where the $N_j^m$ are the usual $C^0$ Lagrange basis functions on $\Delta_m$ (note that $\nabla N_i = -\nabla N_j - \nabla N_k$). Then the right hand side of equation (57) can be written as

$$\sum_{\Delta_m \in T_i} \left( \int_{\partial FV_i^m} \left( \mathbf{D}_i \left( \nabla N_j^m (U_j - U_i) + \nabla N_k^m (U_k - U_i) \right) \right) \cdot \vec{n} d\Gamma \right) \ . \tag{58}$$

Expression (58) may be rewritten as

$$\sum_{\Delta_m \in T_i} \left( \left( \mathbf{D}_i \left( \nabla N_j^m (U_j - U_i) + \nabla N_k^m (U_k - U_i) \right) \right) \cdot \int_{\partial FV_i^m} \vec{n} d\Gamma \right) \ ,$$

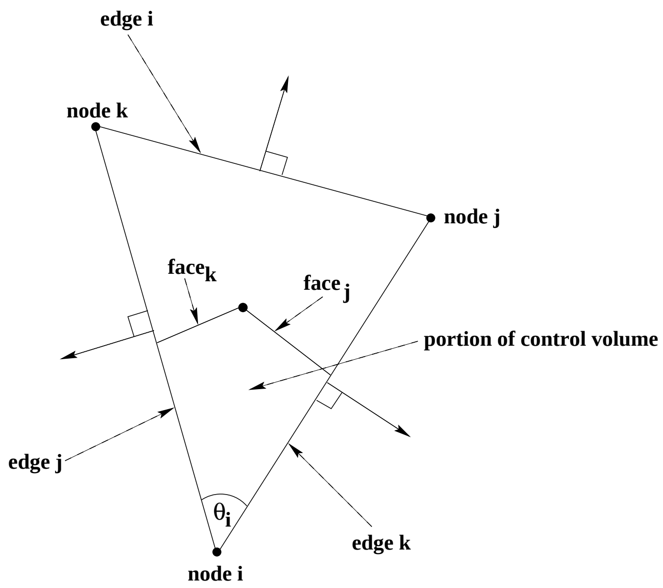


FIGURE 11: *Finite element/volume triangle with control volume.*

which is equal to

$$\sum_{\Delta_m \in T_i} \Bigg[ \left( \mathbf{D}_i \left( \nabla N_j^m (U_j - U_i) + \nabla N_k^m (U_k - U_i) \right) \right) \times \left( \int_{\partial \Gamma^m_{face_j}} \vec{n} d\Gamma^m_{face_j} + \int_{\partial \Gamma^m_{face_k}} \vec{n} d\Gamma^m_{face_k} \right) \Bigg] , \tag{59}$$

where $\Gamma^m_{face_j}$ and $\Gamma^m_{face_k}$ are the portions of the control volume in $\Delta_m$ (see Figure 11). Note that the integrals in (59) are independent of path. Hence, without loss of generality, we can take $\Gamma^m_{face_j}$ and $\Gamma^m_{face_k}$ to be portions of a centroid control volume. In Selmin and Formaggia (1996) it is shown that for centroid control volumes

$$\int_{\partial \Gamma^m_{face_j}} \vec{n} d\Gamma^m_{face_j} + \int_{\partial \Gamma^m_{face_k}} \vec{n} d\Gamma^m_{face_k} = \frac{1}{6} l_i^m \vec{n}_i^m - \frac{1}{6} l_j^m \vec{n}_j^m + \frac{1}{6} l_i^m \vec{n}_i^m - \frac{1}{6} l_k^m \vec{n}_k^m ,$$

where $l_i^m$ is the length of triangle edge $i$ for $\Delta_m$ and $\vec{n}_i^m$ is the outward pointing unit normal to edge $i$ (refer to Figure 11). Thus, expression (59) is equivalent to

$$\sum_{\Delta_m \in T_i} \Bigg[ \left( \mathbf{D}_i \left( \nabla N_j^m (U_j - U_i) + \nabla N_k^m (U_k - U_i) \right) \right) \times \left( \frac{1}{6} l_i^m \vec{n}_i^m - \frac{1}{6} l_j^m \vec{n}_j^m + \frac{1}{6} l_i^m \vec{n}_i^m - \frac{1}{6} l_k^m \vec{n}_k^m \right) \Bigg] . \tag{60}$$

After noting that $\nabla N_i^m = -\frac{l_i^m \vec{n}_i^m}{2|\Delta_m|}$ (see Barth (1994)), where $|\Delta_m|$ is the area of $\Delta_m$, (60) becomes

$$\sum_{\Delta_m \in T_i} \Bigg[ \left(\mathbf{D}_i \left(\nabla N_j^m (U_j - U_i) + \nabla N_k^m (U_k - U_i)\right)\right) \times \\ \left(-\frac{1}{3}\nabla N_i^m + \frac{1}{3}\nabla N_j^m - \frac{1}{3}\nabla N_i^m + \frac{1}{3}\nabla N_k^m\right) |\Delta_m| \Bigg] ,$$

which in turn simplifies to

$$\sum_{\Delta_m \in T_i} \left(\left(\mathbf{D}_i \left(\nabla N_j^m (U_j - U_i) + \nabla N_k^m (U_k - U_i)\right)\right) \cdot (-\nabla N_i^m)|\Delta_m|\right) \tag{61}$$

since $\nabla N_i = -\nabla N_j - \nabla N_k$. Expression (61) equals

$$\sum_{\Delta_m \in T_i} \left( - \int_{\Delta_m} \nabla' N_i^m \mathbf{D}_i \nabla N_j^m d\Omega (U_j - U_i) - \int_{\Delta_m} \nabla' N_i^m \mathbf{D}_i \nabla N_k^m d\Omega (U_k - U_i) \right)$$

which reduces to

$$\sum_{j \in \Omega_i} \int_{\Omega} \nabla' N_i \mathbf{D}_i \nabla N_j d\Omega (U_j - U_i) \ . \tag{62}$$

Expression (62) is the finite volume discretization of the nonconservative diffusion term in equation (4).

# B Local Extremum Diminishing Scheme

In this appendix we will derive the conditions under which the following scheme

$$U_{ij+\frac{1}{2}}^{n+1} = \begin{cases} \frac{1}{2}(U_i^{n+1} + U_j^{n+1}) & \text{if } \vec{L}_{ij} \cdot \mathbf{V}(x_i, y_i) \geq 0 \\ U_{up_{ij}}^{n+1} + \frac{\phi(q_{ij+\frac{1}{2}}^{n+1})}{2}(U_{down_{ij}}^{n+1} - U_{up_{ij}}^{n+1}) & \text{if } \vec{L}_{ij} \cdot \mathbf{V}(x_i, y_i) < 0 \end{cases} \tag{63}$$

with arbitrary temporal weighting on an arbitrary triangular mesh produces a positive coefficient scheme for nonconservative hyperbolic equations such as (47). We will also show that the positivity of coefficients implies that scheme (63) is LED.

To keep the exposition simple, we will consider discretizing the first-order hyperbolic equation(47). The following material can be easily, although tediously, generalized to the case of equation (4). We will simply provide the final result for equation(4).

Discretizing equation (47), along the lines used to derive (45), using scheme (63) gives us

$$
\begin{aligned}
A_i\left(\frac{U_i^{n+1}-U_i^n}{\Delta t}\right) &= \theta\sum_{j\in\Omega_i}\alpha_{ij}[U_i^{n+1}+\frac{\phi(q_{ij+\frac{1}{2}}^{n+1})}{2}(U_j^{n+1}-U_i^{n+1})] \\
&+ \theta\sum_{j\in\Omega_i}\beta_{ij}[\frac{1}{2}(U_i^{n+1}+U_j^{n+1})] \\
&+ (1-\theta)\sum_{j\in\Omega_i}\alpha_{ij}[U_i^n+\frac{\phi(q_{ij+\frac{1}{2}}^{n})}{2}(U_j^n-U_i^n)] \\
&+ (1-\theta)\sum_{j\in\Omega_i}\beta_{ij}[\frac{1}{2}(U_i^n+U_j^n)]\ ,
\end{aligned}
\tag{64}
$$

where $\alpha_{ij} = \min(\vec{L}_{ij}\cdot\mathbf{V}(x_i,y_i),0)$ and $\beta_{ij} = \max(\vec{L}_{ij}\cdot\mathbf{V}(x_i,y_i),0)$. After noting that $q_{ij+\frac{1}{2}}^{n+1} = \frac{U_i^{n+1}-U_{2up_{ij}}^{n+1}}{U_j^{n+1}-U_i^{n+1}}$, equation (64) becomes

$$
\begin{aligned}
A_i\left(\frac{U_i^{n+1}-U_i^n}{\Delta t}\right) &= \theta\sum_{j\in\Omega_i}\alpha_{ij}[U_i^{n+1}+\frac{\phi(q_{ij+\frac{1}{2}}^{n+1})}{2q_{ij+\frac{1}{2}}^{n+1}}(U_i^{n+1}-U_{2up_{ij}}^{n+1})] \\
&+ \theta\sum_{j\in\Omega_i}\beta_{ij}[\frac{1}{2}(U_i^{n+1}+U_j^{n+1})] \\
&+ (1-\theta)\sum_{j\in\Omega_i}\alpha_{ij}[U_i^n+\frac{\phi(q_{ij+\frac{1}{2}}^{n})}{2q_{ij+\frac{1}{2}}^{n}}(U_i^n-U_{2up_{ij}}^n)] \\
&+ (1-\theta)\sum_{j\in\Omega_i}\beta_{ij}[\frac{1}{2}(U_i^n+U_j^n)]\ ,
\end{aligned}
$$

which after collecting terms becomes

$$
\begin{aligned}
A_i\left(\frac{U_i^{n+1}-U_i^n}{\Delta t}\right) &= \theta\sum_{j\in\Omega_i}\left(\alpha_{ij}+\alpha_{ij}\frac{\phi(q_{ij+\frac{1}{2}}^{n+1})}{2q_{ij+\frac{1}{2}}^{n+1}}+\frac{\beta_{ij}}{2}\right)U_i^{n+1} \\
&+ \theta\sum_{j\in\Omega_i}\alpha_{ij}\frac{\phi(q_{ij+\frac{1}{2}}^{n+1})}{2q_{ij+\frac{1}{2}}^{n+1}}(-U_{2up_{ij}}^{n+1}) + \theta\sum_{j\in\Omega_i}\frac{\beta_{ij}}{2}U_j^{n+1} \\
&+ (1-\theta)\sum_{j\in\Omega_i}\left(\alpha_{ij}+\alpha_{ij}\frac{\phi(q_{ij+\frac{1}{2}}^{n})}{2q_{ij+\frac{1}{2}}^{n}}+\frac{\beta_{ij}}{2}\right)U_i^n \\
&+ (1-\theta)\sum_{j\in\Omega_i}\alpha_{ij}\frac{\phi(q_{ij+\frac{1}{2}}^{n})}{2q_{ij+\frac{1}{2}}^{n}}(-U_{2up_{ij}}^n) + (1-\theta)\sum_{j\in\Omega_i}\frac{\beta_{ij}}{2}U_j^n\ .
\end{aligned}
\tag{65}
$$

After letting $\bar{\alpha}_{ij} = \frac{\Delta t}{A_i}\alpha_{ij}$ and $\bar{\beta}_{ij} = \frac{\Delta t}{A_i}\beta_{ij}$, and regrouping terms, equation (65) becomes

$$\left[1+\theta\sum_{j\in\Omega_i}\left(-\bar{\alpha}_{ij}-\bar{\alpha}_{ij}\frac{\phi(q^{n+1}_{ij+\frac{1}{2}})}{2q^{n+1}_{ij+\frac{1}{2}}}-\frac{\bar{\beta}_{ij}}{2}\right)\right]U_i^{n+1} =$$

$$\theta\sum_{j\in\Omega_i}\bar{\alpha}_{ij}\frac{\phi(q^{n+1}_{ij+\frac{1}{2}})}{2q^{n+1}_{ij+\frac{1}{2}}}(-U^{n+1}_{2up_{ij}})+\theta\sum_{j\in\Omega_i}\frac{\bar{\beta}_{ij}}{2}U_j^{n+1}$$
$$+\left[1+(1-\theta)\sum_{j\in\Omega_i}\left(\bar{\alpha_{ij}}+\bar{\alpha_{ij}}\frac{\phi(q^{n}_{ij+\frac{1}{2}})}{2q^{n}_{ij+\frac{1}{2}}}+\frac{\bar{\beta}_{ij}}{2}\right)\right]U_i^n$$
$$+(1-\theta)\sum_{j\in\Omega_i}\bar{\alpha}_{ij}\frac{\phi(q^{n}_{ij+\frac{1}{2}})}{2q^{n}_{ij+\frac{1}{2}}}(-U^{n}_{2up_{ij}})+(1-\theta)\sum_{j\in\Omega_i}\frac{\bar{\beta}_{ij}}{2}U_j^n\ . \quad (66)$$

Note that $\sum_{j\in\Omega_i}(\bar{\alpha}_{ij}+\bar{\beta}_{ij}) = 0$ since $\mathbf{V}$ is always evaluated at node $i$. This is because equation (47) was discretized in nonconservative form and $\oint \vec{n}d\Gamma = \int \nabla(1)d\Omega = 0$. Thus, equation (66) simplifies to

$$\left[1+\theta\sum_{j\in\Omega_i}\left(-\bar{\alpha}_{ij}\frac{\phi(q^{n+1}_{ij+\frac{1}{2}})}{2q^{n+1}_{ij+\frac{1}{2}}}+\frac{\bar{\beta}_{ij}}{2}\right)\right]U_i^{n+1} =$$

$$\theta\sum_{j\in\Omega_i}\left(-\bar{\alpha}_{ij}\frac{\phi(q^{n+1}_{ij+\frac{1}{2}})}{2q^{n+1}_{ij+\frac{1}{2}}}U^{n+1}_{2up_{ij}}+\frac{\bar{\beta}_{ij}}{2}U_j^{n+1}\right)$$
$$+\left[1+(1-\theta)\sum_{j\in\Omega_i}\left(\bar{\alpha_{ij}}\frac{\phi(q^{n}_{ij+\frac{1}{2}})}{2q^{n}_{ij+\frac{1}{2}}}-\frac{\bar{\beta}_{ij}}{2}\right)\right]U_i^n$$
$$+(1-\theta)\sum_{j\in\Omega_i}\left(-\bar{\alpha}_{ij}\frac{\phi(q^{n}_{ij+\frac{1}{2}})}{2q^{n}_{ij+\frac{1}{2}}}U^{n}_{2up_{ij}}+\frac{\bar{\beta}_{ij}}{2}U_j^n\right)\ . \quad (67)$$

Note that $\bar{\alpha}_{ij} \leq 0$, $\bar{\beta}_{ij} \geq 0$ and $\frac{\phi(q^n_{ij+\frac{1}{2}})}{q^n_{ij+\frac{1}{2}}} \geq 0$ (recall property (53)). Hence, in order for all the coefficients in (67) to be positive we need to ensure that

$$(1-\theta)\sum_{j\in\Omega_i}\left(\bar{\alpha}_{ij}\frac{\phi(q^{n}_{ij+\frac{1}{2}})}{2q^{n}_{ij+\frac{1}{2}}}-\frac{\bar{\beta}_{ij}}{2}\right) \geq -1\ .$$

After recalling property (53), this simplifies to

$$\sum_{j\in\Omega_i}\left(-\bar{\alpha}_{ij}\gamma_{ij+\frac{1}{2}}+\frac{\bar{\beta}_{ij}}{2}\right) \leq \frac{1}{(1-\theta)}\ . \quad (68)$$

If condition (68) is met, then all of the coefficients in (67) are positive. By defining

$$U_i^{\max} = \max(U^{n+1}_{k\in\Omega_i}, U^n_{k\in\Omega_i}, U_i^n)$$

and noting that $U^{n+1}_{2up_{ij}}$ is the convex weighting of two $U^{n+1}_{k,\ k\in\Omega_i}$, we can write equation (67) as

$$\left[1+\theta\sum_{j\in\Omega_i}\left(-\bar{\alpha}_{ij}\frac{\phi(q^{n+1}_{ij+\frac{1}{2}})}{2q^{n+1}_{ij+\frac{1}{2}}}+\frac{\bar{\beta}_{ij}}{2}\right)\right]U^{n+1}_i =$$

$$\theta\sum_{j\in\Omega_i}\left(-\bar{\alpha}_{ij}\frac{\phi(q^{n+1}_{ij+\frac{1}{2}})}{2q^{n+1}_{ij+\frac{1}{2}}}+\frac{\bar{\beta}_{ij}}{2}\right)U^{\max}_i$$

$$+\left[1+(1-\theta)\sum_{j\in\Omega_i}\left(\bar{\alpha}_{ij}\frac{\phi(q^{n}_{ij+\frac{1}{2}})}{2q^{n}_{ij+\frac{1}{2}}}-\frac{\bar{\beta}_{ij}}{2}\right)\right]U^{\max}_i$$

$$+(1-\theta)\sum_{j\in\Omega_i}\left(-\bar{\alpha}_{ij}\frac{\phi(q^{n}_{ij+\frac{1}{2}})}{2q^{n}_{ij+\frac{1}{2}}}+\frac{\bar{\beta}_{ij}}{2}\right)U^{\max}_i .$$

This simplifies to

$$\left[1+\theta\sum_{j\in\Omega_i}\left(-\bar{\alpha}_{ij}\frac{\phi(q^{n+1}_{ij+\frac{1}{2}})}{2q^{n+1}_{ij+\frac{1}{2}}}+\frac{\bar{\beta}_{ij}}{2}\right)\right]U^{n+1}_i \le \left[1+\theta\sum_{j\in\Omega_i}\left(-\bar{\alpha}_{ij}\frac{\phi(q^{n+1}_{ij+\frac{1}{2}})}{2q^{n+1}_{ij+\frac{1}{2}}}+\frac{\bar{\beta}_{ij}}{2}\right)\right]U^{\max}_i ,$$

implying $U^{n+1}_i \le U^{\max}_i$. Similarly, if $U^{\min}_i = \min(U^{n+1}_{k\in\Omega_i}, U^{n}_{k\in\Omega_i}, U^n_i)$, then $U^{n+1}_i \ge U^{\min}_i$. Hence, if condition (68) is satisfied then scheme (63) is LED. It is interesting to note that this result holds only when a nonconservative discretization is used, since the velocity ($\mathbf{V}$) is an arbitrary function of the coordinates.

Although similar results can be obtained when the flux limiting scheme (49) is used when either $\vec{L}_{ij}\cdot\mathbf{V}(x_i,y_i) < 0$ or $\vec{L}_{ij}\cdot\mathbf{V}(x_i,y_i) \ge 0$, there are two advantages to using scheme (49) only when $\vec{L}_{ij}\cdot\mathbf{V}(x_i,y_i) < 0$. First, the amount of additional numerical diffusion is reduced. Second, the value of $U^{n+1}_i$ depends only on values at neighbouring nodes, i.e. the value of $U^{n+1}_i$ depends only on the $U^n_{j\in\Omega_i}$ and the $U^{n+1}_{j\in\Omega_i}$. Hence, the nonzero structure of the Jacobian matrix is no different from that resulting when central weighting or first-order upstream weighting is used.

When diffusion is present, scheme (63) can be used. In such cases condition (68) becomes

$$\sum_{j\in\Omega_i}\left(-\bar{\alpha}_{ij}\gamma_{ij+\frac{1}{2}}+\frac{\bar{\beta}_{ij}}{2}\right)-\bar{\eta}_{ii}\le\frac{1}{(1-\theta)} , \tag{69}$$

where $\bar{\eta}_{ii}$ is $\frac{\Delta t}{A_i}\eta_{ii}$. Note that $-\eta_{ii}$ is positive. If condition (69) is met and all the $\eta_{ij}$ are nonnegative, then it can be shown that the scheme is LED. In general, it is not possible to ensure that all the $\eta_{ij}$ will be nonnegative for equation (4) because the diffusion terms are nonconstant. If the $\eta_{ij}$ are not all nonnegative and $U$ satisfies a Lipschitz condition, then it can be shown (see Zvan (1999)) that

$$U^{\min}_i + \mathcal{O}(h) \le U^{n+1}_i \le U^{\max}_i + \mathcal{O}(h) ,$$

where $h$ denotes the mesh spacing, when scheme (63) is used.

If all the $\eta_{ij}$ are nonnegative, then the following scheme

$$U^{n+1}_{ij+\frac{1}{2}} = \begin{cases} \frac{1}{2}(U_i^{n+1} + U_j^{n+1}) & \text{if } \vec{L}_{ij} \cdot \mathbf{V}(x_i, y_i) + \eta_{ij} \geq 0 \\ U^{n+1}_{up_{ij}} + \frac{\phi(q^{n+1}_{ij+\frac{1}{2}})}{2}(U^{n+1}_{down_{ij}} - U^{n+1}_{up_{ij}}) & \text{if } \vec{L}_{ij} \cdot \mathbf{V}(x_i, y_i) + \eta_{ij} < 0 \end{cases} \tag{70}$$

can be used instead of (63). Scheme (70) will be LED when the following condition is satisfied

$$\sum_{\substack{j\in\Omega \\ \alpha_{ij}+\eta_{ij}<0}} -\bar{\alpha}_{ij}\gamma_{ij+\frac{1}{2}} + \sum_{j\in\Omega_i} \frac{\bar{\beta}_{ij}}{2} + \sum_{\substack{j\in\Omega \\ \alpha_{ij}+\eta_{ij}\geq 0}} \frac{\bar{\alpha}_{ij}}{2} - \bar{\eta}_{ii} \leq \frac{1}{(1-\theta)} \ . \tag{71}$$

There are two advantages to using scheme (70) instead of (63) when all the $\eta_{ij}$ are nonnegative. First, the amount of additional numerical diffusion is usually reduced. Second, condition (71) is typically less strict than condition (69).

Although it can only be shown that a scheme will be approximately LED if we have negative $\eta_{ij}$, in this case scheme (70) can be modified to

$$U^{n+1}_{ij+\frac{1}{2}} = \begin{cases} U^{n+1}_{up_{ij}} + \frac{\phi(q^{n+1}_{ij+\frac{1}{2}})}{2}(U^{n+1}_{down_{ij}} - U^{n+1}_{up_{ij}}) & \text{if } \vec{L}_{ij} \cdot \mathbf{V}(x_i, y_i) < 0 \text{ and} \\ & \quad \vec{L}_{ij} \cdot \mathbf{V}(x_i, y_i) + \eta_{ij} < 0 \\ \frac{1}{2}(U_i^{n+1} + U_j^{n+1}) & \text{otherwise ,} \end{cases} \tag{72}$$

in order to use any positive $\eta_{ij}$ in an attempt to reduce the amount of additional numerical diffusion (relative to scheme (63)). Scheme (72) maintains the nonzero structure of the Jacobian matrix which results from central weighting, and reverts to scheme (70) when all the $\eta_{ij}$ are nonnegative. Note that if we were to use scheme (70) when we have negative $\eta_{ij}$, there would be an increase in the number of nonzeros in the Jacobian.

# C Nonconservative Galerkin Approach for Diffusion

In this appendix we will derive the $\eta_{ij}$ in discretization (45) for equation (4) using a Galerkin approach. If $U^n = \sum_j U_j^n N_j$ with $N_j$ being the linear Lagrange basis functions defined on triangles, then performing integration by parts gives

$$\eta_{ij} = -\int_\Omega \nabla'(N_i\mathbf{D})\nabla N_j d\Omega \tag{73}$$

for the nonconservative diffusion in (4). By Green's theorem equation (73) becomes

$$\eta_{ij} = \sum_{\Delta_m\in\Delta_{ij}} \left( -\oint_{\partial\Delta_m} N_i^m \mathbf{D}\nabla N_j^m \cdot \vec{n} d\Gamma \right) \ , \tag{74}$$

where $\Delta_{ij}$ is the set of two triangles which share the common edge $k$ (see Figure 11) and $N_i^m$ is basis function $N_i$ on triangle $m$ ($\Delta_m$). Equation (74) is equivalent to

$$\eta_{ij} = \sum_{\Delta_m \in \Delta_{ij}} \left( -\int_{\Gamma_j^m} N_i^m \mathbf{D} \nabla N_j^m \cdot \vec{n}_j^m d\Gamma_j^m - \int_{\Gamma_k^m} N_i^m \mathbf{D} \nabla N_j^m \cdot \vec{n}_k^m d\Gamma_k^m \right) , \tag{75}$$

where $\Gamma_j^m$ is triangle edge $j$ and $\vec{n}_j^m$ is the outward pointing unit normal to edge $j$ (see Figure 11) for $\Delta_m$. Note that edge $i$ does not appear in equation (75) because $N_i$ is zero along edge $i$. After integrating using the trapezoidal rule, (75) becomes

$$\begin{aligned} \eta_{ij} = & \sum_{\Delta_m \in \Delta_{ij}} \left( -\frac{1}{2} l_j^m (N_{i_i}^m \mathbf{D}_i + N_{i_j}^m \mathbf{D}_j) \nabla N_j^m \cdot \vec{n}_j^m \frac{1}{2} l_k^m (N_{i_i}^m \mathbf{D}_i + N_{i_k}^m \mathbf{D}_k) \nabla N_j^m \cdot \vec{n}_k^m \right) \\ & + \mathcal{O}(h) , \end{aligned} \tag{76}$$

where $l_j^m$ is the length of triangle edge $j$ for $\Delta_m$, $N_{i_j}^m$ is the value of $N_i^m$ at node $j$, $\mathbf{D}_j$ denotes $\mathbf{D}$ evaluated at node $j$ and $h$ is the mesh size parameter. After noting that $N_i^m = 0$ at nodes $j$ and $k$, $\nabla N_j^m = -\frac{l_j^m \vec{n}_j^m}{2|\Delta_m|}$ where $|\Delta_m|$ is the area of triangle $m$, and $N_i^m = 1$ at node $i$, equation (76) becomes

$$\eta_{ij} = \sum_{\Delta_m \in \Delta_{ij}} \left( -\mathbf{D}_i \nabla N_j^m \cdot (-\nabla N_j^m) |\Delta_m| - \mathbf{D}_i \nabla N_j^m \cdot (-\nabla N_k^m) |\Delta_m| \right) + \mathcal{O}(h) ,$$

which is equivalent to

$$\eta_{ij} = -\int_\Omega (-\nabla' N_j - \nabla' N_k) \mathbf{D}_i \nabla N_j d\Omega + \mathcal{O}(h) . \tag{77}$$

After noting that $\nabla N_i = -\nabla N_i - \nabla N_j$, equation (77) becomes

$$\eta_{ij} = -\int_\Omega \nabla' N_i \mathbf{D}_i \nabla N_j d\Omega + \mathcal{O}(h) . \tag{78}$$

Note that in general $\eta_{ij} \neq \eta_{ji}$, which is a consequence of the fact that equation (4) is in nonconservative form.

# References


Arminjon, P. and A. Dervieux (1993). Construction of TVD-like Artificial Viscosities on Two-Dimensional Arbitrary FEM Grids. *Journal of Computational Physics 106*, 176–198.

Barles, G. (1997). Convergence of Numerical Schemes for Degenerate Parabolic Equations Arising in Finance Theory. In L. C. G. Rogers and D. Talay (Eds.), *Numerical Methods in Finance*. Cambridge University Press.

Barraquand, J. and T. Pudet (1996). Pricing of American Path-Dependent Contingent Claims. *Mathematical Finance 6*(1), 17–51.

Barth, T. J. (1994). Aspects of Unstructured Grids and Finite-Volume Solvers for the Euler and Navier-Stokes Equations. In *Lecture Series 1994-05: Computational Fluid Dynamics*. von Karman Institute for Fluid Dynamics.

Barth, T. J. and J. A. Sethian (1998). Numerical Schemes for the Hamilton-Jacobi and Level Set Equations on Triangulated Domains. *Journal of Computational Physics 145*, 1–40.

BIS (1999). The Global OTC Derivatives Market at End-December 1998. Bank for International Settlements, Press release, June 2.

Black, F. and M. Scholes (1973). The Pricing of Options and Corporate Liabilities. *Journal of Political Economy 81*, 637–654.

Blunt, M. and B. Rubin (1992). Implicit Flux Limiting Schemes for Petroleum Reservoir Simulation. *Journal of Computational Physics 102*, 194–210.

Brennan, M. J. and E. S. Schwartz (1977). Convertible Bonds: Valuation and Optimal Strategies for Call and Conversion. *Journal of Finance 32*(5), 1699–1715.

Brennan, M. J. and E. S. Schwartz (1980). Analyzing Convertible Bonds. *Journal of Financial and Quantitative Analysis 15*(4), 907–929.

Chalasani, P., S. Jha, F. Egriboyun, and A. Varikooty (1998). A Refined Binomial Lattice for Pricing American Asian options. 8th Annual Derivatives Securities Conference, Boston.

Cheung, W. and I. Nelken (1994). Costing the Converts. *RISK 7*(7), 47–49.

Ciarlet, P. G. (1978). *The Finite Element Method for Elliptic Problems*. New York: North-Holland Publishing Company.

Coleman, T. F., Y. Li, and A. Verma (1999). Reconstructing the Unknown Local Volatility Function. *The Journal of Computational Finance 2*(3), 77–102.

Cox, J. C., J. E. Ingersoll, Jr., and S. A. Ross (1985). An Intertemporal General Equilibrium Model of Asset Prices. *Econometrica 53*, 363–384.

Crandall, M. G., H. Ishii, and P. L. Lions (1992). User's Guide to Viscosity Solutions of Second Order Partial Differential Equations. *Bulletin (New Series) of the American Mathematical Society 27*(1), 1–67.

Crandall, M. G. and P. L. Lions (1984). Two Approximations of Solutions of the Hamilton-Jacobi Equations. *Mathematics of Computation 43*, 1–19.

Dempster, M. A. H., J. P. Hutton, and D. G. Richards (1998). LP Valuation of Exotic American Options Exploiting Structure. *The Journal of Computational Finance 2*(1), 61–84.

Dewynne, J. N. and P. Wilmott (1995). A Note on Average Rate Options with Discrete Sampling. *SIAM Journal on Applied Mathematics 55*(1), 267–276.

Fleming, W. H. and H. M. Soner (1993). *Controlled Markov Processes and Viscosity Solutions*. New York: Springer-Verlag.

Forsyth, P. A. and H. Jiang (1997). Nonlinear Iteration Methods for High Speed Laminar Compressible Navier-Stokes Equations. *Computers & Fluids 26*, 249–268.

Forsyth, P. A., K. R. Vetzal, and R. Zvan (1999). A Finite Element Approach to the Pricing of Discrete Lookbacks with Stochastic Volatility. *Applied Mathematical Finance 6*, 87–106.

Goodman, J. B. and R. J. LeVeque (1985). On the Accuracy of Stable Schemes for 2D Scalar Conservation Laws. *Mathematics of Computation 45*(171), 15–21.

Harten, A., J. M. Hyman, and P. D. Lax (1976). On Finite-Difference Approximations and Entropy Conditions for Shocks. *Communications on Pure and Applied Mathematics 29*, 297–322.

Ho, T. S. Y. and D. M. Pfeffer (1996). Convertible Bonds: Model, Value Attribution, and Analytics. *Financial Analysts Journal September/October*, 35–44.

Hull, J. C. (1997). *Options, Futures, and Other Derivatives* (Third ed.). Upper Saddle River, New Jersey: Prentice-Hall, Inc.

Hull, J. C. and A. White (1993). Efficient Procedures for Valuing European and American Path-Dependent Options. *The Journal of Derivatives 1 (Fall)*, 21–31.

Ingersoll, Jr., J. E. (1977). A Contingent-Claims Valuation of Convertible Securities. *Journal of Financial Economics 4*, 289–322.

Jackson, N., E. Süli, and S. Howison (1999). Computation of Deterministic Volatility Surfaces. *Journal of Computational Finance 2*(2), 5–32.

Jameson, A. (1995). Positive Schemes and Shock Modelling for Compressible Flows. *International Journal for Numerical Methods in Fluids 20*, 743–776.

Kemna, A. G. Z. and A. C. F. Vorst (1990). A Pricing Method for Options Based on Average Asset Values. *Journal of Banking and Finance 14*, 113–129.

Kröner, D. (1997). *Numerical Schemes for Conservation Laws.* Toronto: John Wiley & Sons Ltd. and B. G. Teubner.

Lawson, C. L. (1977). Software for $C^1$ Surface Interpolation. In J. R. Rice (Ed.), *Mathematical Software III*, pp. 161–193. New York: Academic Press.

LeVeque, R. J. (1990). *Numerical Methods for Conservation Laws.* Basel: Birkhauser Verlag.

Levin, A. (1998). Recovering Implied Volatility and Distribution from American Futures Option Prices Using the Regularization Method. In *Proceedings of Computational and Quantitative Finance '98*, New York.

McConnell, J. J. and E. S. Schwartz (1986). LYON Taming. *Journal of Finance 41*(3), 561–577.

Merton, R. C. (1973). Theory of Rational Option Pricing. *Bell Journal of Economics and Management Science 4 (Spring)*, 141–183.

Nicolaides, R. A. (1992). Direct Discretization of Planar Div-Curl Problems. *SIAM Journal on Numerical Analysis 29*(1), 32–56.

Nyborg, K. G. (1996). The Use and Pricing of Convertible Bonds. *Applied Mathematical Finance 3*, 167–190.

Oleĭnik, O. A. (1957). Discontinuous Solutions of Non-Linear Differential Equations. *Uspekhi Mathematicheskikh Nauk 12*, 3–73. English translation in *American Mathematical Society Translations (Series 2)* 26:95-172, 1963.

Pooley, D. M., P. A. Forsyth, K. R. Vetzal, and R. B. Simpson (1999). Unstructured Meshing for Two Asset Barrier Options. Working paper, University of Waterloo.

Rogers, L. C. G. and Z. Shi (1995). The Value of an Asian Option. *Journal of Applied Probability 32*(4), 1077–1088.

Selmin, V. and L. Formaggia (1996). Unified Construction of Finite Element and Finite Volume Discretizations for Compressible Flows. *International Journal for Numerical Methods in Engineering 39*, 1–32.

Smoller, J. (1994). *Shock Waves and Reaction-Diffusion Equations* (Second ed.). New York: Springer-Verlag.

Spekreijse, S. (1987). Multigrid Solution of Monotone Second-Order Discretizations of Hyperbolic Conservation Laws. *Mathematics of Computation 49*(179), 135–155.

Stulz, R. M. (1982). Options on the Minimum or the Maximum of Two Risky Assets. *Journal of Financial Economics 10*, 161–185.

Sulem, A. (1997). Portfolio Selection with Transaction Costs. In L. C. G. Rogers and D. Talay (Eds.), *Numerical Methods in Finance*. Cambridge University Press.

Sweby, P. K. (1984). High Resolution Schemes Using Flux Limiters for Hyperbolic Conservation Laws. *SIAM Journal on Numerical Analysis 21*(5), 995–1011.

Thuburn, J. (1997). TVD Schemes, Positive Schemes, and the Universal Limiter. *Monthly Weather Review 125*, 1990–1993.

van Leer, B. (1974). Towards the Ultimate Conservative Difference Scheme. II. Monotonicity and Conservation Combined in a Second-Order Scheme. *Journal of Computational Physics 14*, 361–370.

Wilmott, P. (1998). *Derivatives: The Theory and Practice of Financial Engineering*. West Sussex, England: John Wiley & Sons.

Wilmott, P., J. N. Dewynne, and S. Howison (1993). *Option Pricing: Mathematical Models and Computation*. Oxford: Oxford Financial Press.

Zienkiewicz, O. C. (1977). *The Finite Element Method* (Third ed.). Toronto: McGraw-Hill Limited.

Zvan, R. (1999). *The Numerical Solution of Two-Factor PDE Option Pricing Models*. Ph. D. thesis, University of Waterloo. Forthcoming.

Zvan, R., P. A. Forsyth, and K. R. Vetzal (1998a). Penalty Methods for American Options with Stochastic Volatility. *Journal of Computational and Applied Mathematics 91*, 199–218.

Zvan, R., P. A. Forsyth, and K. R. Vetzal (1998b). Robust Numerical Methods for PDE Models of Asian Options. *The Journal of Computational Finance 1*(2), 39–78.

Zvan, R., P. A. Forsyth, and K. R. Vetzal (1999). Discrete Asian Barrier Options. *The Journal of Computational Finance*. To appear.